

Enhancing Energy Sustainability in Coastal Regions: A Proposed Techno-Economic Assessment of a 60 kW Grid-Connected Solar PV System for an Institution in Swarna Dweep, Bangladesh using PVsyst Software

Ayman Khan^a, Abdullah Al Masud^a, Tarek Ahmed^a, Nabil Mohammad Chowdhury^a

^a*Department of Mechanical and Production Engineering, Ahsanullah University of Science and Technology, Dhaka, Bangladesh*

Emails: ayman.khan1971@gmail.com, abdullahmasud0208@gmail.com, tarekahmedaust@gmail.com

Highlighting Points

- This study details the design of a 60 kW grid-connected solar photovoltaic system tailored for a school in Swarna Dweep, employing high-efficiency bifacial modules and smart inverters. Rigorous load demand analysis and solar resource assessments were performed using PVsyst software.
- This study evaluates energy production, performance metrics, and financial feasibility to ensure a thorough understanding of the system's capabilities. Additionally, it aligns with Sustainable Development Goals by providing clean energy access, supporting education, and promoting socioeconomic development while contributing to environmental sustainability through reduced greenhouse gas emissions.
- The project design addresses Swarna Dweep's unique geographical characteristics, including high solar irradiance and coastal climate conditions. It is expected to generate approximately 93,443 kWh annually with a performance ratio of 0.78, ensuring reliable energy provision tailored to the school's needs while considering logistical challenges, such as salt corrosion and intermittent grid access.
- Beyond providing energy, the project fosters local socioeconomic development and promotes sustainable practices within the community. Additionally, it offers a replicable framework that can facilitate the deployment of cost-effective solar PV systems in similar remote areas, thereby advancing renewable energy adoption across Bangladesh.

Abstract

This study presents a comprehensive design and analysis of a 60 kW grid-connected solar photovoltaic (PV) power plant tailored for a school in Swarna Dweep, a remote island community in Bangladesh experiencing significant energy access limitations. The island's unique geographical and environmental context, including high solar irradiance, coastal climate conditions, and logistical constraints, necessitates robust and adaptable system design. The proposed solution utilizes high-efficiency bifacial PV modules and smart inverters to maximize energy generation while minimizing land use. Detailed load demand analysis, coupled with solar resource assessments using tools such as the Global Solar Atlas and PVGIS, inform system sizing and configuration. PVsyst software simulations predict the annual energy production, system losses, performance ratio, and financial returns over a 20-year lifespan, considering module degradation and other real-world constraints. SketchUp facilitates 3D visualization and optimized panel placement for minimal shadowing. The analysis explored the social impact of aligning the project with relevant Sustainable Development Goals, focusing on improved education, clean energy access, and sustainable development within the community. Environmental impact assessment quantifies greenhouse gas emission reductions and other environmental benefits. A financial analysis, including net present value (NPV), internal rate of return (IRR), and levelized cost of energy (LCOE) calculations, demonstrates the project's economic feasibility and potential for revenue generation through net metering. This study provides a replicable framework for deploying sustainable and cost-effective solar PV systems in similar remote or isolated settings.

Keywords: grid-connection, renewable energy integration, Remote Island electrification, energy optimization, economic analysis, simulation.

1. Introduction

Bangladesh is a densely populated South Asian country that faces mounting energy demands while simultaneously tackling environmental challenges and relying on fossil fuels [1]. The growing global demand for energy, coupled with the depletion of fossil fuel resources and the urgent need to mitigate climate change[2], has highlighted the critical importance of renewable energy solutions. Solar photovoltaic (PV) systems have emerged as promising alternatives [3], offering clean [4], reliable, and cost-effective energy. Among the various applications, grid-connected solar PV systems stand out for their ability to integrate seamlessly with existing utility grids [5]. These systems not only reduce dependency on conventional energy sources, but also help minimize energy costs by allowing surplus energy to be fed back into the grid. Schools, in particular, are ideal candidates for solar PV adoption [6] because they typically have large rooftop areas for installation, consistent daytime energy demands, and a central role in fostering environmental awareness.

The proposed solar PV power plant in Patenga demonstrates the viability of solar energy in addressing both local energy needs and contributing to the national power grids [7]. Such projects align with Bangladesh's commitment to the United Nations Sustainable Development Goals (SDGs) [8], fostering economic growth, sustainable infrastructure, and environmental conservation. With solar PV technology becoming more cost-effective and efficient [9], Bangladesh is positioned to harness this renewable energy source to transition toward a greener and more resilient energy future, reduce its carbon footprint, and promote energy security [10].

Swarna Dweep, a remote coastal island with high solar irradiance and growing energy needs, represents a compelling case for the implementation of solar PV systems [11]. The school on the island has been grappling with energy supply challenges owing to its reliance on conventional power sources, which are often disrupted by logistical and infrastructural constraints. Integrating a grid-connected solar PV system can not only meet the school's electricity requirements, but also contribute surplus energy to the local grid, reducing reliance on fossil fuels while promoting sustainable development. Using solar resource data [12], the potential of a high-performance PV system on Swarna Dweep can be optimized through site-specific design and analysis.

Research in developing countries has highlighted the transformative potential of solar PV systems in addressing energy deficits and reducing costs. Shirzad et al. [13] analyzed a 34.98 MW solar PV plant in Kandahar, Afghanistan, using the PVsyst software to optimize energy production and system performance. The plant generates 54,000 MWh annually with a 79% performance ratio, leveraging abundant solar resources (4.86 kWh/m²/day) and optimization techniques such as tilt angle adjustments. Similarly, Bouroumeid et al. [14] studied a 12 MW system in Sidi Bel Abbès, Algeria, producing 23,000 MWh annually with a 75% performance ratio. This study addressed temperature and sunlight fluctuations and proposed maintenance strategies, such as cleaning and cooling, to mitigate losses.

Educational institutions are increasingly adopting solar photovoltaic (PV) systems to reduce energy costs and promote sustainability. Krishna et al. [15] explored a 400 kWp rooftop system at the Bapatla Engineering College, India, meeting 80% of the institution's energy needs, with an annual output of 624 MWh and an 81.5% performance ratio. Similarly, Trivaldo et al. [16] planned a 13.875 kWp system for a school in Indonesia, achieving a 75% performance ratio and generating 20 MWh annually. This study underscored the feasibility of small-scale systems tailored to specific environmental conditions, with a payback period of 12.5 years. Dey and Subudhi [17] designed a 90 kW rooftop system at NIT Rourkela, India, producing 15.67 MWh per subsystem annually, saving \$135,000, and reducing CO₂ emissions by 2,199.6 tons over 30 years.

Rooftop PV systems offer significant environmental and economic benefits in urban and institutional settings. Akpolat et al. [18] assessed a system for Marmara University, Turkey, which generated 34 MWh annually with a 79% performance ratio, reducing CO₂ emissions by 30 tons per year. Gharibshahian I et.al. [19] evaluated a 100 kW grid-connected system in Semnan City, Iran, producing 178.99 MWh annually with an 83% performance ratio, while offsetting 171 tons of CO₂ over 30 years. Mohanty and Srivalli [20] optimized the design of a rooftop system for a college in Bhubaneswar, India, using the System Advisor Model (SAM) to address shadow effects and tilt angles, demonstrating how advanced modeling tools can enhance system performance.

Solar PV systems face unique challenges in regions with extreme climates. Aoun analyzed a 20 MW plant in Adrar, Algeria, which achieved a 72% performance ratio under harsh conditions, emphasizing regular maintenance to counter thermal losses [21]. Raxmatov et al. [22] evaluated a 300 kW system at Bukhara State University, Uzbekistan, generating 486.8 MWh over eight months with a 76% performance ratio and a 9.7-year payback period. These studies collectively demonstrate the adaptability of solar PV systems to diverse scales and environments, thereby offering cost-effective and sustainable energy solutions.

Despite significant advancements in solar photovoltaic (PV) systems, research gaps remain in addressing unique challenges posed by specific environments, such as remote coastal regions like Swarna Dweep, where issues like logistical constraints, salt corrosion, and intermittent grid access are prevalent. Although studies have focused on grid-connected and standalone systems, hybrid approaches combining solar PV with other renewables or storage solutions remain underexplored, particularly for small communities and educational settings. Additionally, although advanced tools such as PVsyst and SAM are widely used for performance optimization, their applicability under extreme conditions or real-world constraints, such as maintenance limitations and policy barriers, are not fully understood. Economic analyses have primarily targeted mid-to high-income regions, leaving gaps in the understanding of the feasibility of deploying cost-effective PV solutions in low-income areas with limited resources. The proposed system seeks to address these gaps while enhancing the accuracy and effectiveness of solar grid design.

The objectives of this study are as follows:

1. To design and implement a 60 kW grid-connected solar photovoltaic system that meets the school's energy needs, ensuring a reliable and sustainable power supply.
2. To reduce the school's carbon footprint by utilizing renewable energy and supporting environmental sustainability goals.
3. To optimize the energy costs and operational efficiency through net metering, excess energy is fed back into the grid and generates potential revenue.

This study explores the design and development of a 60 kW grid-connected solar photovoltaic (PV) power plant to provide sustainable and reliable electricity to a school in Swarna Dweep, Bangladesh, a remote island community facing significant energy access challenges. The proposed system aims to ensure reliable electricity supply while promoting renewable energy adoption in educational institutions. Advanced solar technologies, including high-efficiency bifacial panels and smart inverters, are used to optimize energy generation. The design is informed by a detailed demand analysis and site-specific resource assessments utilizing tools such as the Global Solar Atlas and PVGIS for optimal panel placement, tilt, and orientation. The initiative also evaluates social, environmental, and financial impacts, highlighting its potential to reduce greenhouse gas emissions, lower operational costs, and provide additional revenue through net metering. This project not only ensures a stable learning environment, but also serves as a replicable model for deploying renewable energy systems in remote areas. The feasibility and benefits of solar PV systems in addressing energy challenges are demonstrated by aligning them with Bangladesh's renewable energy goals and global sustainable development targets.

2. Methodology

This study aimed to assess the solar energy potential and design a ground-mounted PV system using a systematic methodology, as shown in **Figure 1**. Pre-data analysis will be performed using the Global Solar Atlas, and geographical data will be sourced from PVGIS to evaluate solar irradiation, which is critical for estimating the energy generation. PVsyst was used to simulate the system's performance, evaluating energy yield, losses, efficiency, and financial returns over the project's duration, based on environmental and system parameters. In addition, SketchUp creates a 3D model to optimize the layout and orientation. These tools ensure accurate analysis and visualization and provide valuable insights into the feasibility and performance of the proposed PV system.

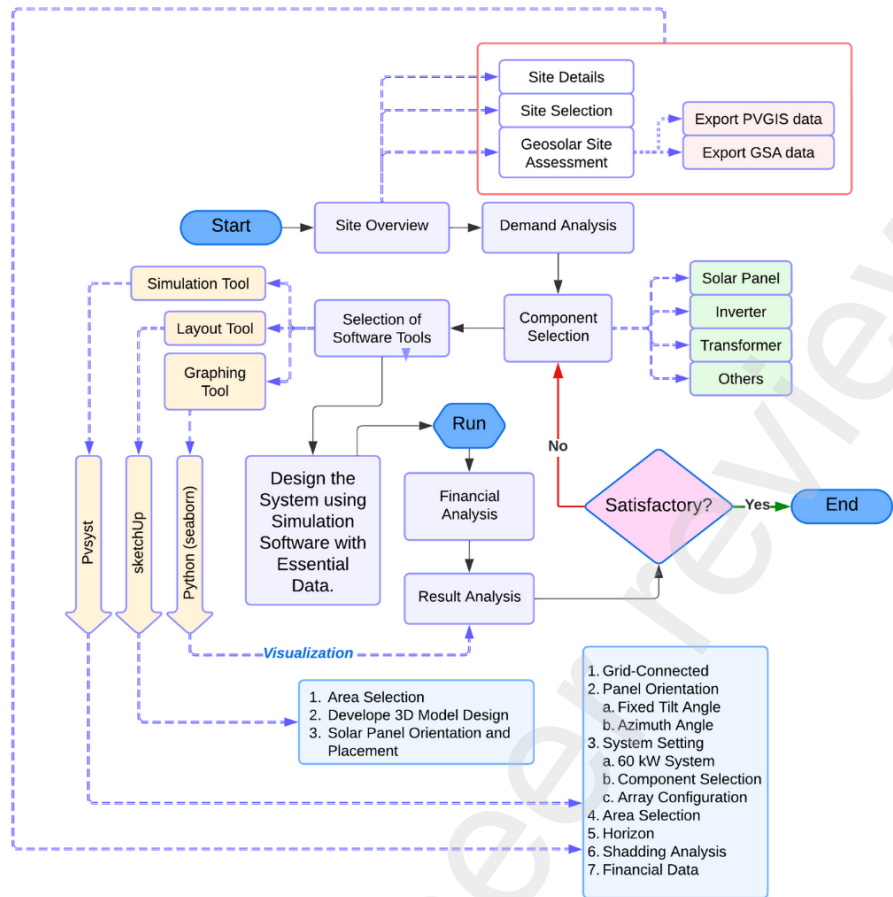


Figure 1: Flowchart of proposed methodology

3. Site Overview

3.1 Site Details

Swarna Dweep, also known as Jahaijar Char, is a 360 square kilometer island in the Meghna estuary, part of the Hatiya Upazila under Noakhali District, Bangladesh. Administered by the Bangladesh Army as a strategic training base, the site offers abundant sunlight because of its tropical location, making it ideal for ground-mounted solar power plants. However, the coastal environment presents challenges, such as high humidity, cyclonic winds, and salt spray, necessitating robust design considerations for durability. Existing infrastructure, including cyclone shelters and agricultural projects, provide logistical support for solar facilities. The island's development initiatives, such as fish farming and planned tourism, highlight potential future energy demands and underscore the project's relevance and potential impact.

3.2 Site Selection

The proposed grid-connected solar photovoltaic power plant was strategically located at coordinates 22.544417° N, 91.303639° E, as depicted in [Figure 2](#). This site was meticulously selected using the Global Solar Atlas (GSA) and PVGIS tools to ensure high photovoltaic power output while being proximate to schools and other institutions, thereby minimizing transmission losses and reducing infrastructure costs. The area boasts substantial global irradiation levels, an optimal dry-bulb temperature range for photovoltaic panel efficiency, and favorable wind and diffuse radiation conditions, all of which enhance the plant's performance and sustainability. This well-

considered site selection underscores a project's commitment to efficient and long-term power generation, laying a robust foundation for its success.



Figure 2: Location of the Solar Power Plant Site

3.3 Geosolar Assessment

The geographical data for the proposed grid-connected solar photovoltaic (PV) power plant in Swarna Dweep ensures the system's efficiency and reliability. The assessment involves evaluating the solar resource potential at the site, considering the geographical location, climate, and other environmental factors. A Photovoltaic Geographical Information System (PVGIS), developed by the European Commission's Joint Research Centre, was employed to simulate and assess the solar resources at the site. The weather data for a TMY for Swarna Dweep using PVsyst were validated against the PVGIS-SARAH database for Global Horizontal Irradiation and Horizontal Diffuse Irradiation. [Figure 3](#) shows a clear resemblance in how similar the data remain throughout the year.

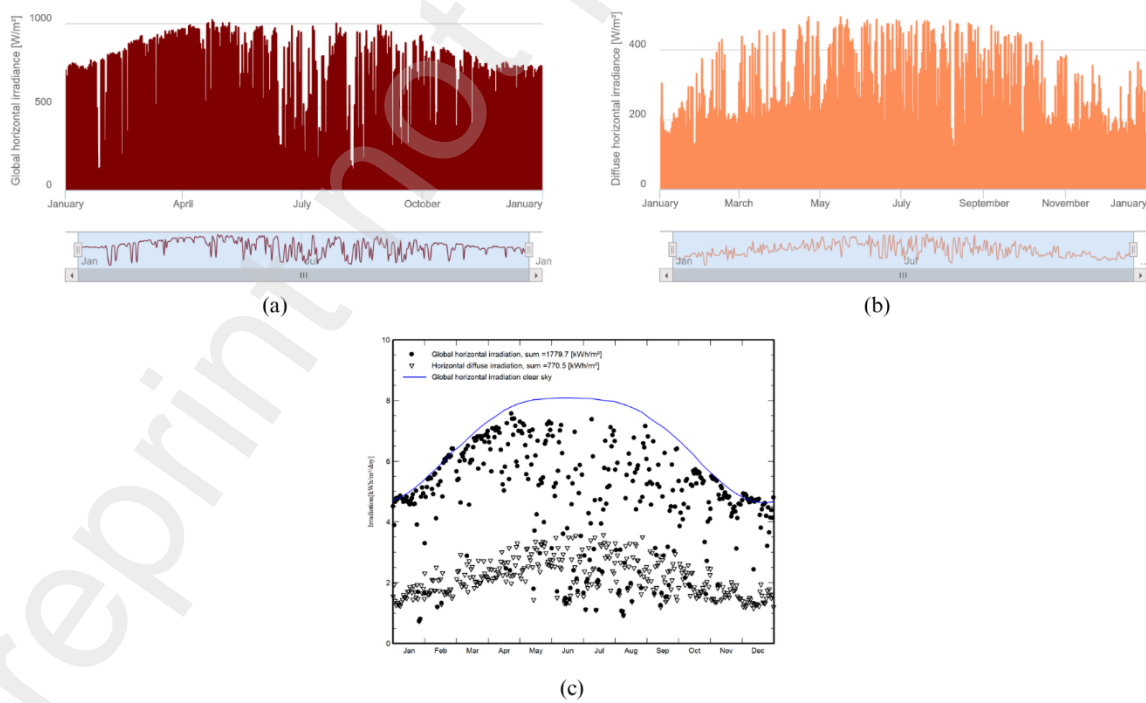


Figure 3: Typical Meteorological Year (TMY) Data for Swarna Dweep: (a) and (b) from PVGIS database, (c) from PVsyst

The pre-simulation using the PVGIS tool revealed an optimal slope angle of 27° and an azimuth angle of 7° for the solar panels, which are crucial for maximizing in-plane irradiation. In-plane radiation is important because it directly influences the energy capture efficiency of PV modules. The yearly PV energy production was estimated to be 89,333.73 kWh, with a yearly in-plane irradiation of 1,979.73 kWh/m². These figures indicate a robust solar resource potential at the site despite a total system loss of 24.79%, which is within the acceptable parameters for the region.

The analysis also identified July as the critical month for solar resource availability, with a monthly in-plane irradiation of 132.98 kWh/m², as shown in **Figure 4**. However, the hourly irradiance data for the month showed sufficient solar energy during the school's operational hours (8:00 AM to 2:00 PM), with irradiance ranging from 163.74 W/m² to 496.33 W/m² as illustrated in **Table 1**. This suggests that the system can meet the school's energy requirements even during periods of lower solar irradiance.

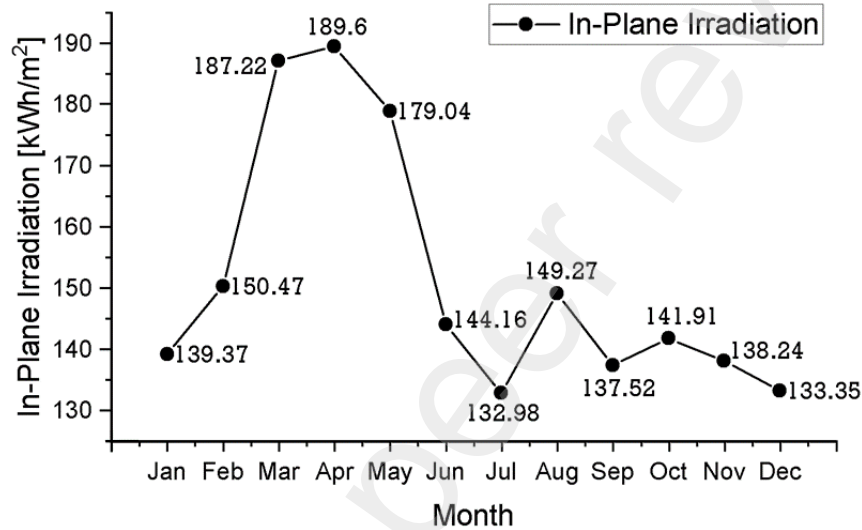


Figure 4: Monthly In-Plane Radiation at Fixed Angle (2005 - 2016)

Table 1: Hourly Global Horizontal Irradiance of July

Time (UTC+6)	GlobHor (W/m ²)
8:00	163.74
9:00	285.31
10:00	405.76
11:00	484.26
12:00	534.99
13:00	546.21
14:00	496.33
15:00	403.76
16:00	300.63

Various important monthly irradiation data are illustrated in **Figure 16 (a)**, which highlights the significant variation in solar energy availability throughout the year. The temperature data from the PVGIS-SARAH database indicated a relatively stable temperature range throughout the year, with an average of 26.21°C during the peak solar hours at an altitude of 2 m, as shown in **Figure 16 (c)**. This is crucial for predicting the performance of PV modules because temperature variations can affect their efficiency.

The solar path diagram in [Figure 7](#) is crucial for optimizing solar project design. Analysis using the diagram enables precise determination of the ideal panel orientation and tilt for maximum irradiance capture, while also facilitating accurate shading analysis to minimize potential energy losses. This information is particularly important in environments with potential obstructions, allowing for strategic array placement for optimal system efficiency.

4. Demand Analysis

4.1 Load Demand

Load demand analysis is a critical initial step in designing solar photovoltaic (PV) power systems. It provides insights into the energy consumption patterns, peak load requirements, and overall electrical needs, which are essential for ensuring an efficient and reliable power supply. For the proposed school in Swarna Dweep, this analysis involved cataloging all electrical appliances, their power ratings, and their usage patterns. The analysis included 388 appliances distributed across various areas of the school, including administrative offices, classrooms, laboratories, and support facilities. These appliances range from basic lighting and fans to more power-intensive equipment, such as air conditioners and laboratory apparatus. Based on this, we calculated the hourly energy production for each appliance by using the following formula:

$$\text{Hourly Energy (W)} = \frac{\text{Total Energy (wh)}}{\text{Operating Hours}} \Rightarrow [\text{Eq 1}]$$

Table 2 illustrates the appliance-wise power distribution across six hourly intervals, offering a granular view of energy utilization patterns. This breakdown not only facilitates the identification of peak load periods but also highlights the diversity in appliance power consumption. The detailed categorization, spanning high-consumption devices such as air conditioners and ovens to low-power equipment like CC cameras and mesh Wi-Fi, underscores the complexity of load management in the proposed system.

Table 2: Hourly Power Consumption of Appliances

Appliance	8-9 h (W)	9-10 h (W)	10-11 h (W)	11-12 h (W)	12-13 h (W)	13-14 h (W)
Light Bulb	1800	1800	1800	1800	1800	1800
Fan	320	320	320	320	320	320
AC	-	-	13195	13195	13195	-
Refrigerator	170	170	170	170	170	170
TV Station	-	150	-	150	-	-
Digital Display Board	-	-	300	300	-	-
Sound Box	-	-	720	720	-	-
Mesh Wifi	44.64	44.64	44.64	44.64	44.64	44.64
Printer	1420	-	1420	-	1420	-
Computer	2562	2562	2562	2562	2562	2562
Light Bulb	8100	8100	8100	8100	8100	8100
Fan	7200	7200	7200	7200	7200	7200
Digital Display Board	4500	4500	4500	4500	4500	4500
Light Bulb	1080	-	1080	-	1080	1080
Fan	1200	-	1200	-	1200	1200
Computer	-	4270	4270	4270	4270	-

Light Bulb	-	120	120	120	120	-
Fan	-	160	160	160	160	-
Light Bulb	-	360	360	360	360	-
Fan	-	640	640	640	640	-
Light Bulb	180	180	180	180	180	180
Exhaust Fan	200	200	200	200	200	200
Light Bulb	18	18	18	18	18	18
Fan	160	160	160	160	160	160
Exhaust Fan	40	40	40	40	40	40
Monitor	40	40	40	40	40	40
CC Camera	22.5	22.5	22.5	22.5	22.5	22.5
Pump	-	164.12	-	-	164.12	-
Exhaust Fan	-	10	-	-	10	-
Fan	-	-	320	-	-	-
Water Filter	80	80	80	80	80	80
Coffee Maker	820	820	820	820	820	820
Oven	-	-	-	1300	-	-
Total Watt (<i>W</i>)	29957	32131.26	49722.14	47792.14	48876.26	28537.14
Total Kilowatt (<i>kW</i>)	29.957	32.13126	49.72214	47.79214	48.87626	28.53714

The analysis reveals a maximum instantaneous power demand of approximately 53,024.14 watts and a cumulative daily energy consumption of 237,016.08 watt-hours. These figures are crucial for designing a solar PV system that can meet the energy needs of schools.

4.2 Daily Load Curve

The daily load curve provides a comprehensive view of energy consumption patterns throughout a typical school day. **Figure 5** shows the hourly energy consumption from 8 AM to 2 PM for various areas of the school, with a notable peak demand period from 10 AM to 1 PM, coinciding with core school activities.

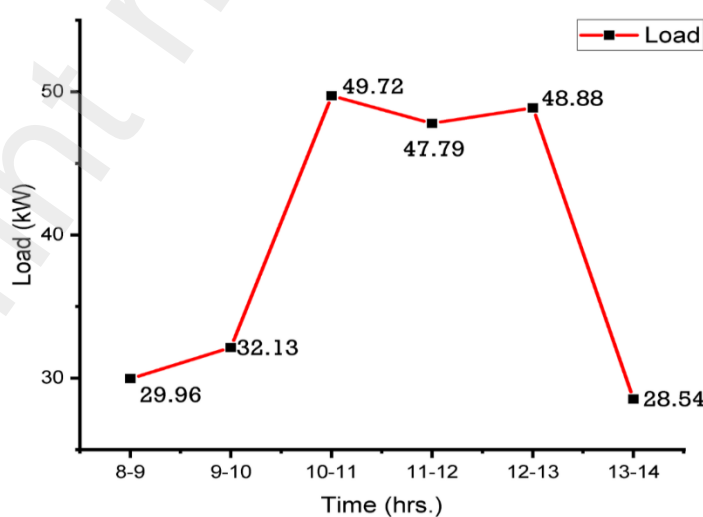


Figure 5: Load Curve Based on Work Hours

This analysis is essential for designing a system capable of handling peak loads and ensuring reliable power supply throughout the day. The insights gained from the load demand and daily load curve analyses are crucial for optimizing solar PV systems and implementing effective energy management strategies.

5. Overall System

5.1 Component Sizing

5.1.1 System Sizing

To determine the appropriate size of the solar system, we first calculated the average sun-hours throughout the year, ensuring sufficient electricity generation even during months with the least amount of sunlight. The average sun hours were computed using Equation (2).

$$\text{Average Sun Hours} = \frac{\text{Daily Average Sun Hours in Summer} + \text{Winter} + \text{Monsoon}}{3} \Rightarrow [\text{Eq 2}]$$

Table 3: Seasonal Sun Hours in Swarna Dweep, Noakhali

Season	Months	Sun Hours	Seasonal Average (Hours)
Winter	November – February	4.60, 4.30, 4.50, 5.37	4.69
Summer	March – June	6.04, 6.32, 5.78, 4.81	5.74
Monsoon	July – October	4.29, 4.82, 4.58, 4.58	4.57

The data for seasonal sunhours in Swarna Dweep are presented in **Table 3**. The summer months (March-June) exhibited the highest average sun hours (5.74 hours), followed by winter (4.69 hours) and monsoon (4.57 hours). To account for variability, we conservatively estimated 4 sun hours for the system design, as July had the lowest sun hours.

Based on a daily energy demand of 240 kWh (rounded up from 237.02 kWh to account for design margins), the system size was calculated using Equation 3, which gives me 60 kW [23].

$$\text{System Size (kW)} = \frac{\text{Daily Energy Demand (kWh)}}{\text{Average Sun Hours}} \Rightarrow [\text{Eq 3}]$$

This solar capacity was designed to generate sufficient electricity to meet the daily energy demand of 240 kWh, accounting for seasonal variations in sunlight. The design ensures consistent energy production even during periods of lower irradiance, enhancing the resilience and economic viability of the system.

5.1.2 Inverter Sizing

Inverter sizing is critical for efficiently converting the DC power from solar panels to AC power for appliance use. The maximum rated power of the system for all appliances is approximately 54 kW. To determine the inverter capacity, we first calculate the total electrical load using the following formula:

$$\text{Total Electrical Load (VA)} = \frac{\text{Maximum Rated Power (W)}}{\text{Power Factor (P.F)}} \Rightarrow [\text{Eq 4}]$$

A power factor of 0.95 is used, as recommended by Global Sustainable Energy Solutions (GSES) in their published article, was used. This factor reflects the efficiency of modern electrical appliances under normal operating conditions.

Next, the inverter capacity is determined using the following formula:

$$\text{Inverter Capacity (VA)} = \frac{\text{Total Electrical Load (VA)} \times \text{Correction Factor}}{\text{Inverter Efficiency}} \Rightarrow [\text{Eq 5}]$$

A correction factor of 1.25 is applied, which is within the industry-standard range of 1.2 to 1.3, provides a safety margin for temporary overloads and future system expansion [24]. The inverter efficiency was assumed to be 95%, which is a typical value for modern inverters.

Using **Equations 4 and 5**, the required inverter capacity was calculated as 75 kVA. To ensure reliability and accommodate potential future growth, an 80 kVA inverter, specified as 80 kW, was selected. This sizing ensures that the inverter can handle the maximum electrical load with a safety margin, thereby enhancing system reliability and longevity.

5.1.3 Transformer Sizing

The selection of an appropriate transformer is critical for seamlessly integrating a solar photovoltaic (PV) system with an electrical grid. The transformer ensures proper voltage matching and maintains the power quality, which is essential for efficient grid interaction. Given the system's inverter-rated power of 80 kW and an adjustable power factor range of 0.8 leading to 0.8 lagging (as specified in the inverter datasheet), the transformer must be capable of handling the inverter's output under various power factor conditions.

$$\text{Transformer Capacity (kVA)} = \frac{\text{Inverter Rated Power (kW)}}{\text{Minimum Power Factor}} \Rightarrow [\text{Eq 6}]$$

This calculation using **Equation 6** indicates that a 100 kVA transformer is necessary to ensure that it can handle the full output of the inverter, even at the minimum power factor of 0.8. This sizing is crucial for maintaining power quality and adhering to grid integration standards.

5.2 Selection of Components

5.2.1 Solar Panel

The JA Solar JAM72D42-620/LB monocrystalline modules with a peak power output of 620 Wp were chosen for their ability to maximize the energy yield while minimizing the number of modules required. This selection optimizes space utilization and reduces installation costs.

The panels feature an N-type bifacial design, which enhances energy capture from both sides, leading to a higher energy yield and lower degradation rates. The solar cell efficiency (η) and fill factor of the panels were 22.2% and 0.75, respectively, as calculated using **Equations 7 and 8**, respectively.

$$\eta = \frac{W_p}{G \times A} \Rightarrow [\text{Eq 7}]$$

$$\text{Fill factor} = \frac{V_{mp} \times I_{mp}}{V_{oc} \times I_{sc}} \Rightarrow [\text{Eq 8}]$$

Thin-film technology modules were not considered because of their lower efficiency and durability compared to crystalline silicon-based panels. The selected panels comply with the IEC 61215 and IEC 61730 standards, ensuring the impact of mechanical, electrical, and thermal stresses on the power output and safety qualification. These panels are well suited to Bangladesh's environmental conditions, offering long-term performance and reliability.

5.2.2 Inverter

The Growatt MAX 80KTL3 LV inverter was selected for its alignment with the calculated inverter capacity requirement of 80 kW for the 60 kW solar installation. As the nearest BSTI-approved option, it provides a slight capacity buffer, thereby ensuring optimal system performance. The inverter features an efficiency rate of 99 %, surpassing the initially considered 95%, thereby minimizing energy losses and enhancing the overall system efficiency. The robust design includes comprehensive protection mechanisms and grid-tie functionality. The compliance with IEC standards further underscores its suitability for this application.

5.2.3 Transformer

We selected the $3\varnothing$ 100 KVA 11/0.415KV transformer from the BSEC approved list as it precisely matches our 100 kVA requirement. This transformer is essential for stepping down the voltage from 11 kV to 415 V, making it compatible with the grid and output of our chosen Growatt inverter. The selection strictly adheres to SREDA's guidelines for grid integration, ensuring seamless power distribution and compliance with local regulations. It was used as a step-up transformer.

5.2.4 Others Accessories

Installing String Combiner Box (SCB) aggregates the output from multiple strings of solar panels into a unified DC output. The net meter accurately measured the electricity consumed by the grid and the surplus electricity generated by the solar system that was fed back into the grid. For the lighting arresters, we positioned one on the primary, high-voltage side of the transformer to guard against direct strikes and surges on the incoming power lines. The other is placed on the secondary, low-voltage side to protect the downstream solar equipment, including inverters and combiner boxes. Installing solar panels at a 27-degree tilt angle requires two critical components: column supports and fasteners. For column supports, each string includes two 20-meter base columns, costing 351.35 USD (41,259 BDT) per column, and ten 2-meter angle support columns, costing 8.78 USD (1,031 BDT) each. With seven strings in total, the cost of the columns is calculated as $(2 \times 7 \times 41,259) + (2 \times 10 \times 7 \times 1,031) = 721,966$ BDT. Fasteners were required to secure these columns [25]. Each 20-meter column needs four fasteners per string at 1 USD (117.43 BDT), while the 2-meter columns require two fasteners per pair, costing 6 USD (704.58 BDT) per string. For seven strings, the total cost of the fasteners was $(4 \times 7 \times 117.43) + (2 \times 10 \times 7 \times 6 \times 117.43) = 101,929$ BDT. A side view of our ground-mounted solar panel based on the column and fastener placement is shown in [Figure 6](#).

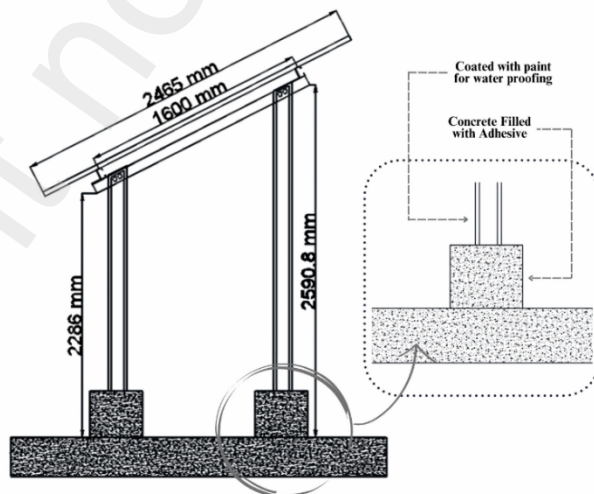


Figure 6: Schematic Diagram of Ground Mounting using AutoCAD

5.3 Number of Modules

In this study, a solar module with a capacity of 620 Wp per panel was used to achieve the target capacity of 60 kW. The performance of the 60 kW solar PV system was analyzed using the Photovoltaic Geographical Information System, which is a fast, easy, and reliable tool for evaluating the performance of both grid-connected and standalone PV systems [26]. The number of modules required was calculated as follows:

$$\text{Number of Modules} = \frac{60,000 \text{ W}}{620 \text{ W}} \approx 97$$

The PVsyst optimization yielded a 98-module array configured in seven strings of 14 modules each, achieving a 1.06 Pnom ratio with no overload loss. Efficient string distribution across five MPPT inputs utilizes three SCBs: a 1/1 single string (SCB), two-string 2/2 SCB (), and a 4/2 SCB (four strings combined into two outputs (SCB)). This setup optimizes MPPT functionality by assigning individual strings to three MPPT inputs and paired strings to the remaining two [27]. A grid-connected configuration was chosen because it allows for the offset of grid electricity consumption and the potential for revenue generation through feed-in tariffs, which incentivize the export of solar-generated electricity to the grid [26].

5.4 Panel Pitch Assessment

The solar panel layout was optimized using a solar path diagram, focusing on the solar elevation and azimuth angles at 8 am and 2 pm, respectively. These times align with the school's operating hours, ensuring maximum efficiency during critical sunhours.

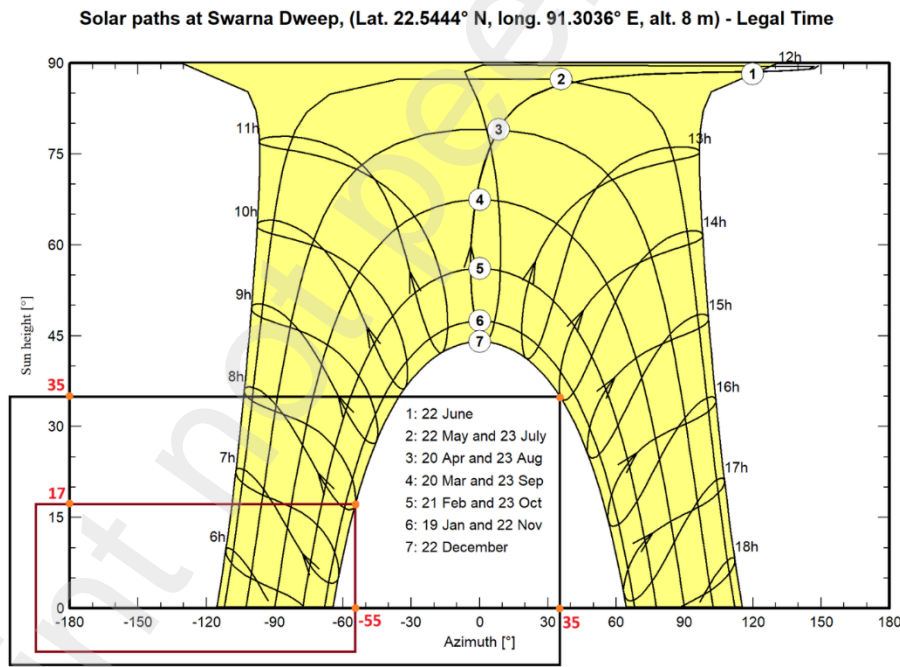


Figure 7: Elevation & Azimuth Angles using Solar Path Diagram at extreme points (8h and 14h)

As shown in **Figure 7**, at the extreme point of 8 h, the elevation angle was 17°, and the azimuth angle was 55°. At the extreme point at 14 h, the elevation angle was 35° and the azimuth angle was 35°.

To optimize sunlight exposure and minimize shading, the inter-row spacing and pitch were calculated using panel datasheet specifications, solar path diagram data, and appropriate formulas:

$$1. Ht = L x \sin (\beta) \Rightarrow [\text{Eq 9}]$$

$$2. Hp = L x \cos (\beta) \Rightarrow [\text{Eq 10}]$$

$$3. D_s = L \sin(\beta) \tan(\alpha_s) \Rightarrow [\text{Eq 11}]$$

$$4. S = D_s \times \sin(\gamma_s) \Rightarrow [\text{Eq 12}]$$

$$5. Pitch = H_p + S \Rightarrow [\text{Eq 13}]$$

Where:

α_s = Solar Elevation Angle (radian)

γ_s = Solar Azimuth Angle (radian)

β = Tilt Angle (radian)

H_t = Panel Height

H_p = Horizontal Projection

D_s = Shadow Distance of the panel

S = Inter-Row Spacing

Table 4 was calculated using the formulas (**Equations 9-13**) outlined in the preceding sections. The PVsyst report also indicates a shading limit angle ($\gamma_{shading}$) of 20°, ensuring that an 8-hour timeline provides optimal sunlight exposure without shading. This finding was further validated by considering a solar elevation angle of 17°, confirming the efficiency of the system under these conditions [28].

Table 4: Calculation of Inter-Row Spacing and Pitch for Optimal Panel Placement

Landscape setup								
Tilt Angle, β	Length, L	Panel Height, H_t	Horizontal Projection, H_p	Solar Elevation Angle, α_s	Shadow Distance Panel, D_s	Solar Azimuth Angle, γ_s	Inter-Row Spacing, S	Pitch
27	1.136	0.52	1.013	17	1.7008	55	1.39	2.41
Portrait setup								
Tilt Angle, β	Length, L	Panel Height, H_t	Horizontal Projection, H_p	Solar Elevation Angle, α_s	Shadow Distance Panel, D_s	Solar Azimuth Angle, γ_s	Inter-Row Spacing, S	Pitch
27	2.467	1.12	2.199	17	3.6634	57	3.07	5.28

The angles are in *degrees* and the rest are in *meter*

A portrait setup for solar panels is recommended as landscape orientation can render bypass diodes ineffective, reducing power output by up to 92%, and potentially damaging PV modules [29]. In addition, portrait installations typically require fewer mounting rails and brackets, resulting in lower material and labor costs.

5.5 Area Selection

Precise area calculations are essential for accurate system design and simulation, ensuring that the predicted electricity generation aligns with actual performance.

The selected solar panel had dimensions of 2.467 m × 1.136 m (with a 2 mm tolerance). A 50 mm inter-panel spacing allows for connections and separation [30]. For a 27° tilt angle, the pitch was approximately 5.3 m. The

proposed 98-module array (per PVsyst) has dimensions of ~32 m (length; 5.3 m × 6) and ~17 m (width; 1.136 m × 14 + 0.05 m × 13), resulting in a total array area of ~544 m² (32 m × 17 m) using Eq 14 [31].

$$\text{Area of Total Solar Panels} = \int_0^L \int_0^W dA \Rightarrow [\text{Eq 14}]$$

where L and W are the length and width, respectively.

5.6 Wiring Setup

5.6.1 Wiring Length

The solar panel array consists of seven strings, each 20 m in length, which are selected considering the safety margin and various losses for wiring [32]. These strings were connected to three SCBs: SCB 4/2, SCB 2/2, and SCB 1/1. The wiring within each string and from the strings to the SCBs is critical for ensuring an optimal performance. Each string comprising the solar panels is connected in series, with both positive and negative wiring running along the length of the string.

Table 5 presents the wiring configuration and lengths of the solar panel strings and their corresponding Solar Control Boxes (SCBs). The specified distances, such as the 9-meter measurement, denote the one-way distance from the closest end of each string to the SCB. All calculations were optimized to ensure that no additional wire was required, thereby enhancing material efficiency.

Table 5: Wiring Lengths for Solar Panel Strings and SCBs

Wiring Path	Number of Strings	Distance per Connection (m)	Wiring per meter (m)	Total Wiring Length (m/ft)
Start to End of Single Array	7	20	40	280 / 919
End of Single Array to SCB 4/2	4	9	18	72 / 236
End of Single Array to SCB 2/2	2	9	18	36 / 118
End of Single Array to SCB 1/1	1	9	18	18 / 59
Total			58	406 / 1332

Notes:

- For both positive and negative wiring, we must multiply by 2.
- All distances and wiring lengths were provided in meters and feet for international readability.

We need to determine power, voltage, and current in a solar power plant, encompassing solar panels, string combiner boxes (SCBs), inverters, transformers, and grid connection. The process involves data collection from manufacturer datasheets, application of relevant formulas, and consideration of operational conditions.

For further analysis, **Table 6** will be used to determine the power, voltage, and current specifications of various components required for designing the 60 kW solar system.

Table 6: Technical Data of PV module and Inverter

Table a

PV Module	
Manufacturer	JA SOLAR
Model	JAM72D42-620/LB
Unit Nom. Power	620 Wp
Nominal (STC)	60.8 kWp

Imp	14.25 A
Vmp	43.51 A
Cell	Mono-16BB
No. of Cells	144 (6 × 24)
Dimensions	2465 ± 2mm × 1134 ± 2mm × 35 ± 1mm
Weight	34.6 kg
Module Efficiency	22.2 %
Rated Max Power (Pmax) at 10% Solar Irradiation ratio	670 W
Wire Gauge	12 AWG

Table b

Inverter	
Manufacturer	GROWATT
Model	MAX 80KTL3 LV
Dimensions (W/H/D)	860/600/300 mm
Weight	86 kg
Unit Nominal Power	80.0 kWac
Pnom ratio	1.06
Input Data (DC)	
Max. voltage	1100 V
Nominal voltage	600 V
MPPT voltage range	200-1000 V
No. of MPP trackers	7
Max current per MPPT	26 A
Max short - circuit current per MPPT	32 A
Output Data (AC)	
Nominal voltage range	340-440 V
Max. output current	128.8 A
Max. efficiency	99 %

5.6.2 Voltage and Current Calculations for Wiring Design

- **Solar Panels:** Each panel has a maximum power current (Imp) of 14.25 A and a maximum power voltage (Vmp) of 43.51 V. For a string of 14 panels, the total voltage is approximately 609.14 V ($43.51 \text{ V} \times 14$), with the current remaining at 14.25 A. The peak power each panel generates is 620 Wp.
- **SCBs:** Three types of String Combiner Boxes (SCBs) were utilized: 1/1 SCB, 2/2 SCB, and 4/2 SCB. Since the 1/1 SCB and 2/2 SCB each use a single string, the current and voltage are identical to the solar panel specifications. For the 4/2 SCB, as four input strings are converted into two strings, the current becomes the current becomes 28.5 and and the voltage remains same.
- **Inverter:** It converts DC power to AC power. Rated for five MPPT channels, each handling 26 A, yielding a total current of 130 A ($26 \text{ A} \times 5 \text{ MPPT channels}$).
- **Transformer:** A three-phase, 100 KVA transformer with a voltage rating of 11/0.415 kV is used as a step-up transformer for the project. The three-phase current is calculated using $(I = \frac{S}{\sqrt{3} \cdot V \cdot PF})$. Here, S is the apparent power (100 KVA), V is the line voltage (11 kV), and PF is the power factor (0.8). The system is considered to operate at full load, ensuring components handle their maximum rated capacities. One study revealed that although the distribution transformer (DT) was not overloaded, it required load

balancing to ensure optimal performance [33]. To accurately analyze the parameters of an energized 11/0.415 kV distribution transformer, it is essential to employ specialized tools and equipment designed for precise data acquisition [34]. So, it is important to monitor the power factor to maintain optimal performance [35].

- **Net Meter:** The same formula as the transformer is used to find the current and voltage.

We have selected copper for electrical wiring due to its high conductivity, durability, and corrosion resistance, making it ideal for efficient and reliable power transmission. Using **Table 7**, we can find out which wire sizes are appropriate based on resistance and ampacity, ensuring minimal energy loss and safe current carrying capacity for each wiring [36], [37]. The table of wire resistance and ampacity values allows for accurate wire selection by matching the required current and voltage drop to the appropriate wire gauge.

Table 7: Wire Gauge (AWG) Specifications for Copper Element

AWG	Copper wire			
	Length-Specific Resistance, R (Ω/kft)	Ampacity at Temperature Rating		
		60 °C	75 °C	90 °C
4/0	0.04901	195	230	260
3/0	0.0618	165	200	225
2/0	0.07793	145	175	195
1/0	0.09827	125	150	170
1	0.1239	110	130	145
2	0.1563	95	115	130
3	0.197	85	100	115
4	0.2485	70	85	95
6	0.3951	55	65	75
8	0.6282	40	50	55
10	0.9989	30	35	40
12	1.588	20	25	30
14	2.525	15	20	25
16	4.016	12	16	18
18	6.385	10	14	16

To find the maximum voltage drop, we have considered a 2% voltage drop for all wirings, adhering to the recommendation that voltage drops in electrical systems, including solar installations, should not exceed 3%, as specified in IEC 60364 Part 52 [38]. This limit ensures efficient operation and minimizes energy loss during the transport and distribution of electrical energy. All calculations of current and voltage for each wiring, including the maximum voltage drop, are summarized in **Table 8**. Using the formulas displayed in **Table 9**, we have calculated the maximum allowable resistance (R_{max}) and compared the results with the length-specific resistance (R) to find out which AWG to use for each wiring based on $R < R_{max}$ and $I < I_{60^{\circ}C}$.

Table 8: Wiring Parameters and Voltage Drop Criteria for Wire Gauge Selection

Case	Wiring (Source to Destination)	Load Current, I (A)	Voltage, V (V)	One-Way Distance, D (m/ft)	V_{drop} (max) (V)
1	Single String to SCB	14.25	609.14	58 / 191	12.1828
2	SCB 4/2 to Inverter	28.5	609.14	25 / 83	12.1828
3	SCB 2/2 to Inverter	14.25	609.14	25 / 83	12.1828
4	SCB 1/1 to Inverter	14.25	609.14	25 / 83	12.1828

5	Inverter to Transformer	130	600	150 / 493	12
6	Transformer to Net Meter	5.25	11000	30 / 98.5	220
7	Net Meter to National Grid	5.25	11000	2883 / 9459	220
8	Net Meter to School	5.25	11000	2883 / 9459	220

Table 9: Wire Gauge Selection Based on Resistance and Ampacity

Parameter	Case 1 (Single Phase)	Case 2 (Single Phase)	Case 3,4 (Single Phase)	Case 5 (Three Phase)	Case 6 (Three Phase)	Case 7, 8 (Three Phase)
Formula Used to find, R_{max}	$\frac{V_{drop(max)} \times 1000}{2 \times I \times D}$	Same as Case 1	Same as Case 1	$\frac{V_{drop(max)} \times 1000}{\sqrt{3} \times I \times D}$	Same as Case 5	Same as Case 5
Max Allowable Resistance, $R_{max}(\Omega/kft)$	2.2380	2.6042	5.1502	0.1081	245.808 ₇	8.392
Selected Wire Size	12 AWG	10 AWG	16 AWG	1/0 AWG	18 AWG	18 AWG

The accuracy of the calculation for case 1 can be confirmed by cross-referencing the results with the data provided in [Table 6a](#). This allows for more reliable validation by ensuring consistency between the calculated values and the reference values in the table.

With the wire sizes determined for each segment of the system, we can now calculate the total cost of wiring by referencing locally available prices for the selected wire gauges. These prices, specific to the region, allow for an accurate estimation of material costs, ensuring the budget aligns with market rates which is detailed in [Table 10](#).

Table 10: Price Estimation for Selected AWG Wire Sizes as a Function of Total Distance

Selected Wire Size	12 AWG	10 AWG	16 AWG	1/0 AWG	18 AWG	Total Price (BDT)
Total Distance, $D_t(m)$	812	25	50	150	5796	
Price (BDT)	138040	4750	7500	105000	695520	950810

6. Layout Design

This section outlines the design of a 60 kW on-grid solar PV system for Swarna Dweep, focusing on technical feasibility, operational efficiency, and site-specific adaptability.

The block diagram in [Figure 8](#) illustrates the energy flow from the PV modules to the grid, highlighting essential components such as the string combiner box (SCB), inverters, protection devices, and the net meter for seamless grid integration. The electrical grid design shown in [Figure 9](#) provides a detailed schematic of the system's configuration, including the arrangement of PV strings, SCBs, MPPT-integrated inverters, and transformers, ensuring optimal power delivery to both the grid and the school. [Figure 10](#) features a 3D visualization developed in SketchUp, offering a clear view of the system's spatial layout, including the placement of PV arrays, SCBs, and the transformer, optimizing the use of available space. Together, these elements depict a well-integrated, efficient solar PV system tailored to the specific needs of Swarna Dweep.

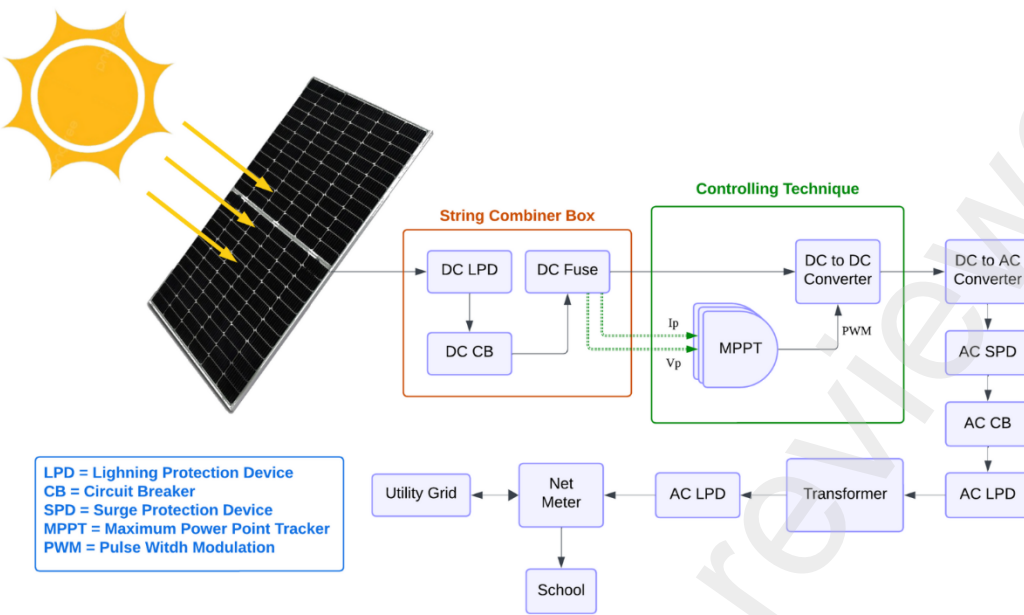


Figure 8: Block Diagram of 60 kW On-Grid Solar PV System

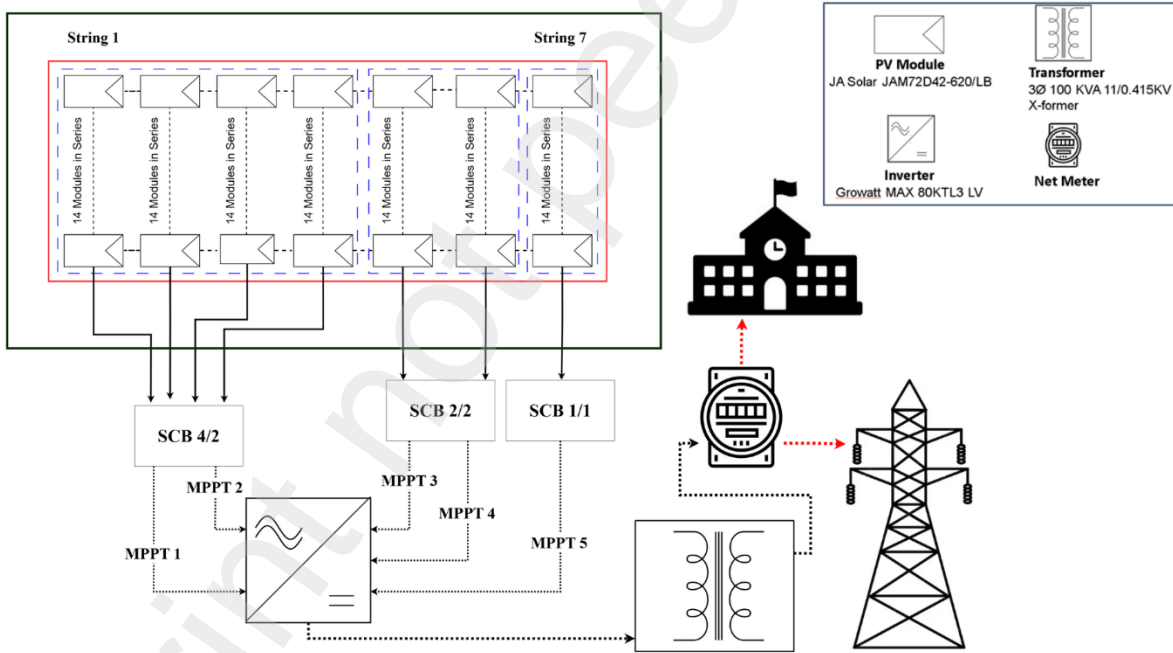


Figure 9: Electrical Grid Design for a 60kW On-Grid Solar System at Swarna Dweep

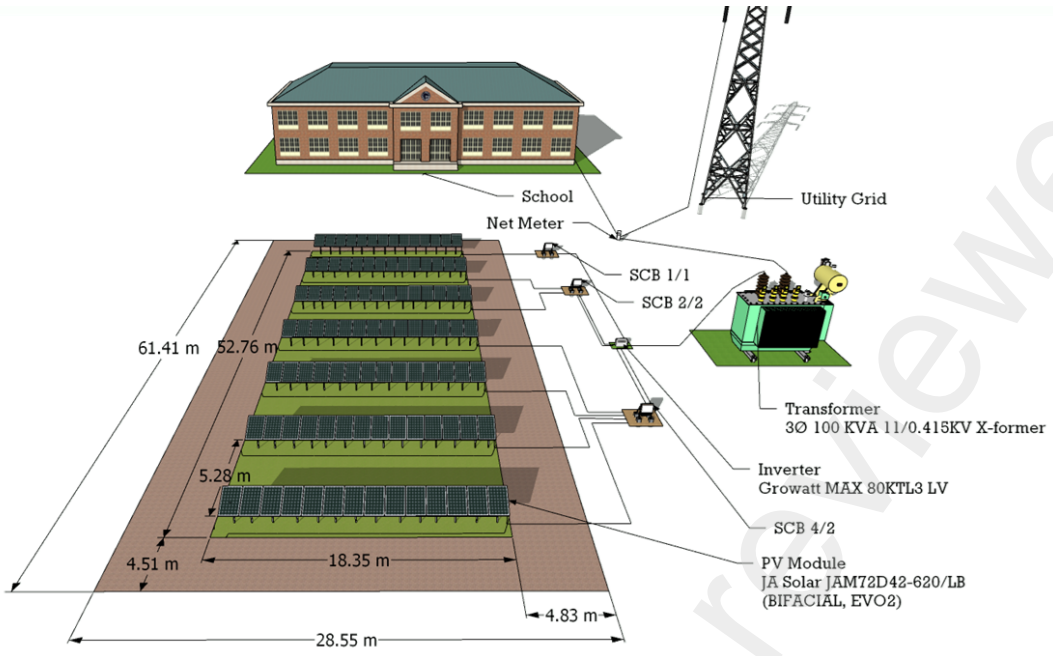


Figure 10: 3D Visualization of a 60 kW On-Grid Solar PV System Design for Swarna Dweep using SketchUp

7. Analysis

7.1 Performance Analysis

The analysis evaluates the solar system's performance, focusing on key metrics such as Normalized Production, Performance Ratio, and energy output trends over 20 years. It highlights system efficiency, the impact of aging, and energy flow losses, providing valuable insights into long-term performance, potential degradation, and overall system reliability.

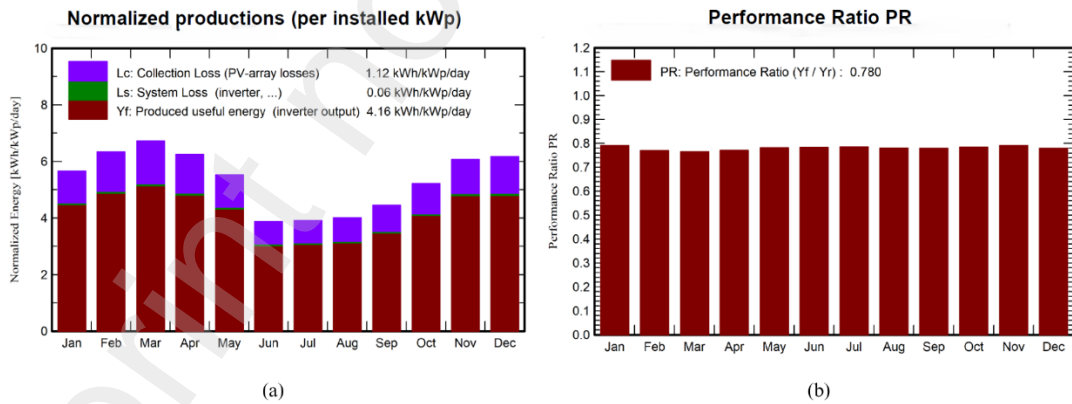


Figure 11: Normalized Production (a) and Performance Ratio (b) throughout the year

In **Figure 11**, we can discern that the solar plant exhibits seasonal variations, with peak energy output in March and the lowest in July. Collection losses increase during summer, while system losses remain stable throughout the year as depicted in Figure 10a. In addition, **Figure 11(b)** shows a consistent performance ratio (PR) of 0.78 indicating steady efficiency in converting solar radiation to electricity [39].

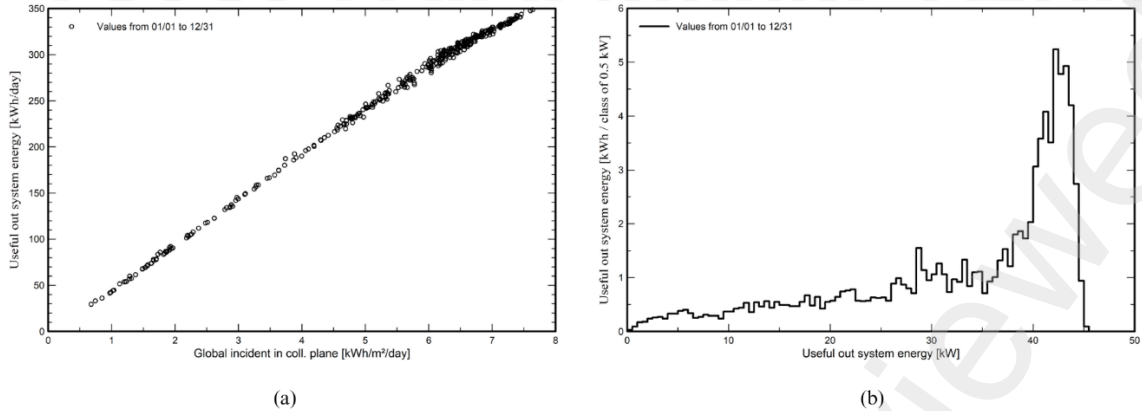


Figure 12: Daily Input/Output Diagram (a) and System Output Power Distribution (b) throughout the year

The daily input-output diagram reveals a strong positive correlation between incident radiation and system energy output, indicating high efficiency which is shown in [Figure 12](#). The system output power distribution graph shows a typical right-skewed pattern, reflecting the plant's ability to handle varying production levels with the potential for high output on optimal days.

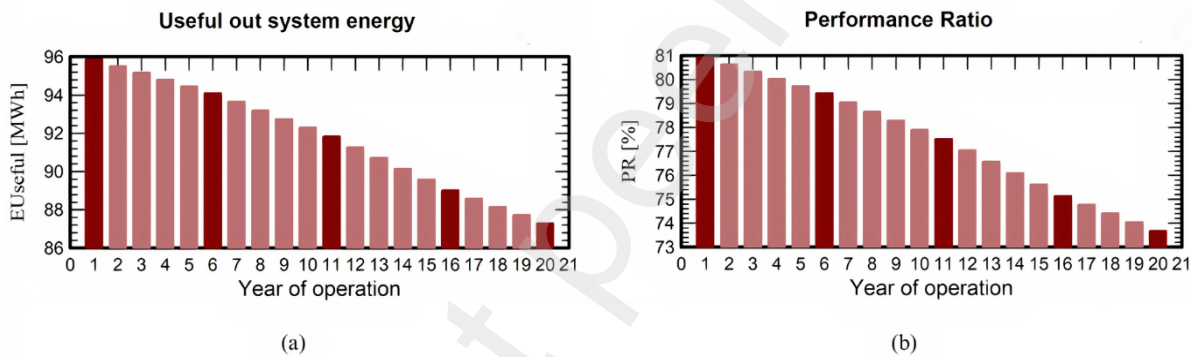


Figure 13: 20-Year Trends in Energy Output (a) and Performance Ratio (b) for a Solar Plant through Aging Process

The solar plant demonstrates a stable and acceptable performance decline over 20 years, with a consistent useful energy output and a PR that remains within expected limits, indicating a well-maintained and reliable system which is illustrated in [Figure 13](#) [39], [40].

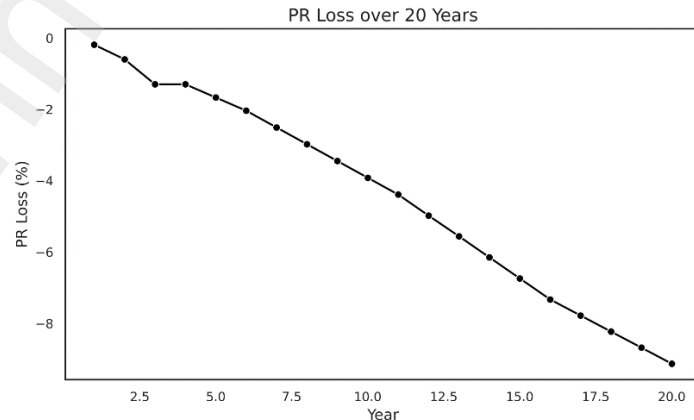


Figure 14: PR Loss (%) Trend Over 20 Years

The graph from [Figure 14](#) indicates a steady decline in system performance due to aging and degradation. While the loss progression appears typical for solar systems, the total PR loss of approximately 9% over two decades is relatively low, suggesting the system is well-maintained and designed [41]. These findings highlight a well-designed system capable of adapting to seasonal changes, offering insights for optimization.

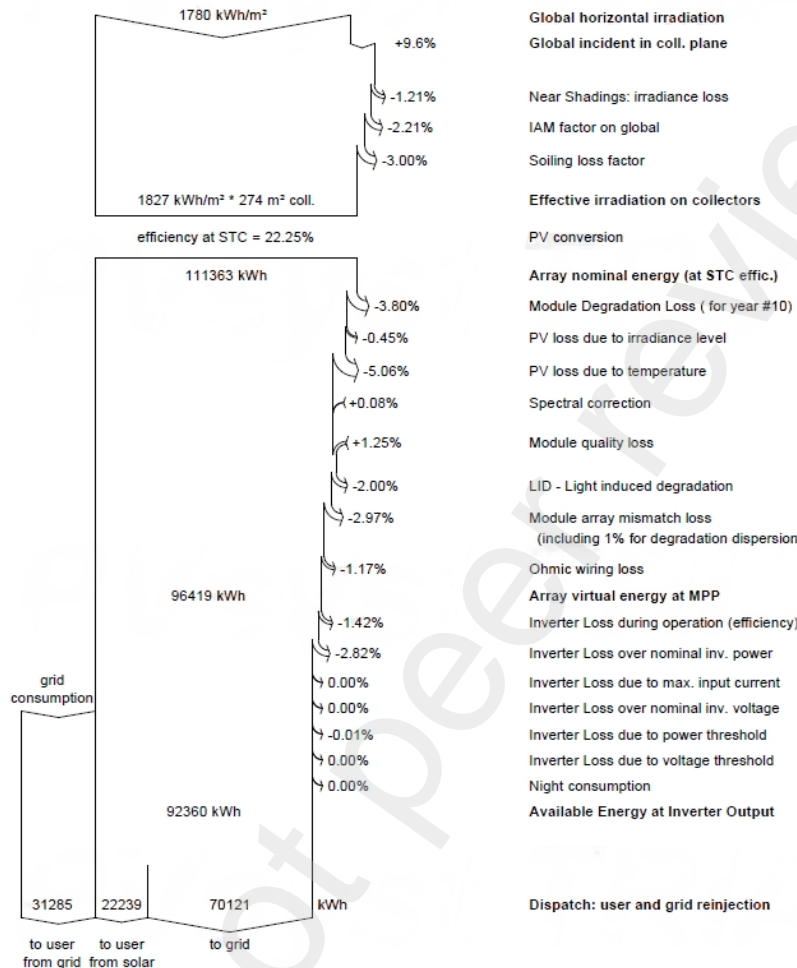
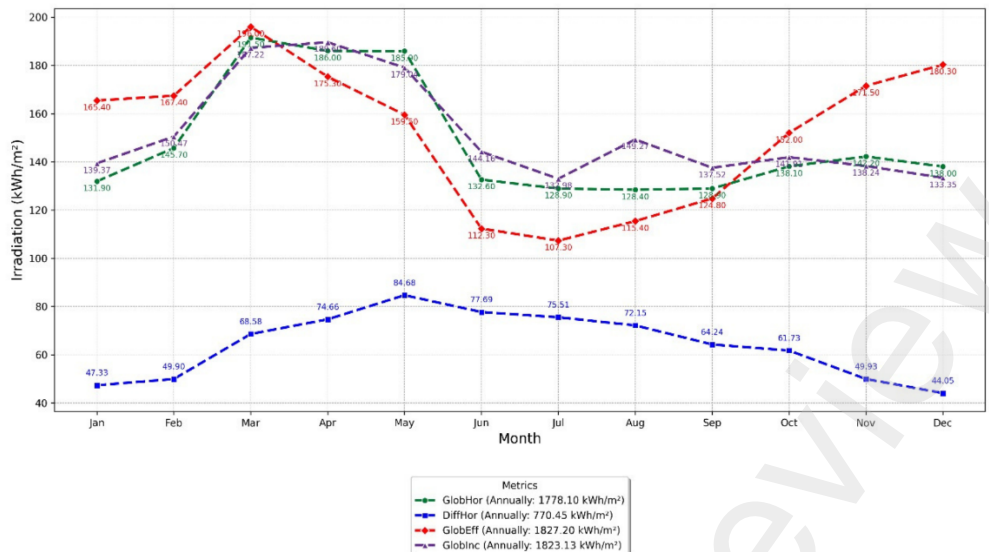
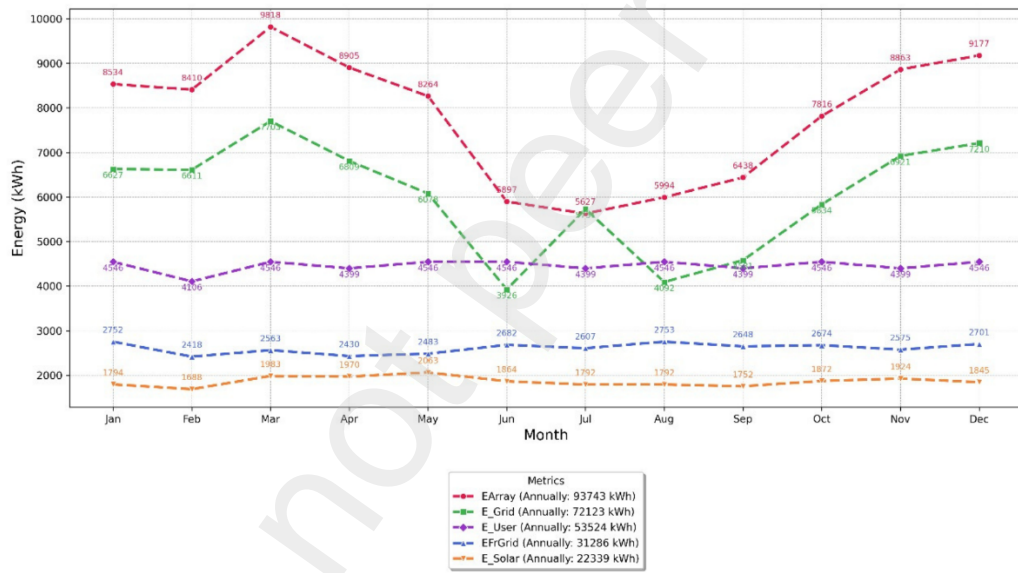


Figure 15: Energy Flow and Loss Distribution (%) in 60 kW Solar Plant

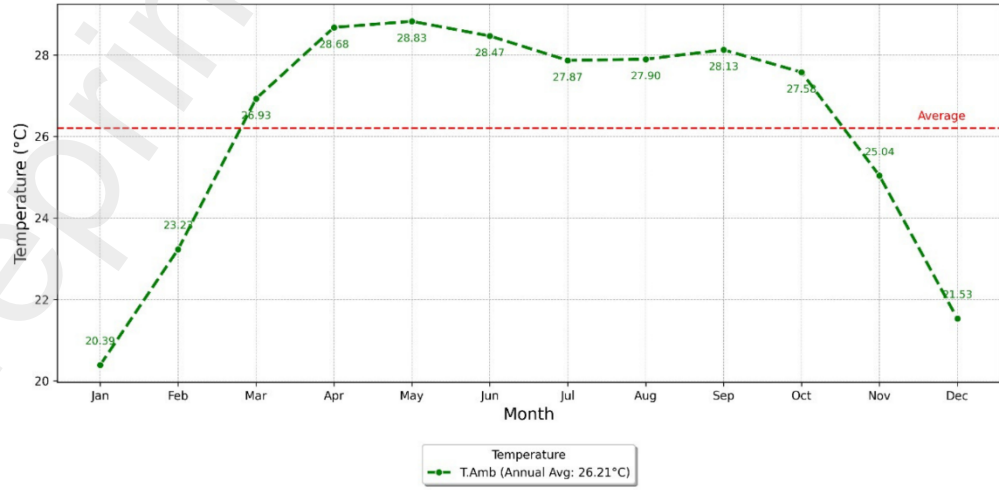
The global horizontal irradiation of 1780 kWh/m² is enhanced to 1827 kWh/m² on the collectors, due to optimal tilt and orientation optimizing energy capture. With a 22.2% SPV conversion efficiency, the nominal annual production is 111,363 kWh, reduced to 96,419 kWh at the maximum power point (MPP) due to inefficiencies. From [Figure 16 \(b\)](#), we found that the array has produced 93,742 kWh of usable electrical energy at its output. The energy distribution which is illustrated in [Figure 15](#) shows that 92,360 kWh is at the inverter output, with 70,121 kWh exported to the grid, 22,239 kWh used by the consumer, and 31,265 kWh imported from the grid, indicating effective net metering which can be sold afterward. The PV system experiences daily losses of 1.12 kWh/kWp (array) and 0.06 kWh/kWp (system). Over 20 years, total array losses reached 15.7%, primarily due to soiling (3.0%), module mismatch (2.0%), light-induced degradation (2.0%), and DC wiring (1.5%), partially offset by a -1.3% module quality gain. Long-term losses include 8.0% from module degradation and 0.4% from mismatch dispersion. IAM loss factors reveal efficiency declines at high incidence angles ($>60^\circ$), guiding optimal panel orientation to reduce losses. Our 27° tilt angle generally aligns the panels to optimize energy capture at a location's latitude, reducing the frequency and impact of high incidence angles around solar noon. Spectral correction coefficients improve accuracy in energy output predictions under varying atmospheric conditions.



(a)



(b)



(c)

Figure 16: Main results and system balance for a 60 kW on-grid solar PV system in Swarna Dweep, highlighting: (a) various types of irradiations, (b) energy contributions from different sources, and (c) ambient temperature trends

7.2 Financial Analysis

Regarding financial analysis, the details of the installation costs and operating costs are included in **Table 11** and **12** respectively.

Table 11: Installation Cost

Component	Quantity (No. of units)	Total Cost (BDT)
PV module	98	10010
Inverter	1	751660
Other components		
Column & Fastener	1022	823895
Wiring	6833 meters	950810
Combiner Box	3	53000
Net Meter	1	30000
Monitoring System	1	40000
Surge arrester	2	3000
Studies and analysis		
Engineering	4	320000
Administration Fees	2	160000
Environmental studies	2	160000
Economic analysis	2	160000
Installation		
Global installation cost per module	98	98000
Global installation cost per inverter	1	30000
Transport	8	120000
Settings	4	60000
Grid connection	1	500000
Total (BDT)		4270375
Depreciable Asset (BDT)		2338554

Table 12: Operating Cost

Item	Total (BDT/year)
Maintenance	
Provision for Inverter Replacement	26845
Salaries	150000
Repairs	60000
Cleaning	30000
Security fund	40000
Subsidies	-20000
Total (OPEX)	286845
Total (including inflation 9.72%)	795783.28

Despite the initial financial burden, the solar photovoltaic power plant project shows a clear recovery phase followed by steady growth in both yearly net profit and cumulative cash flow as we can see from the graph provided in **Figure 17**.

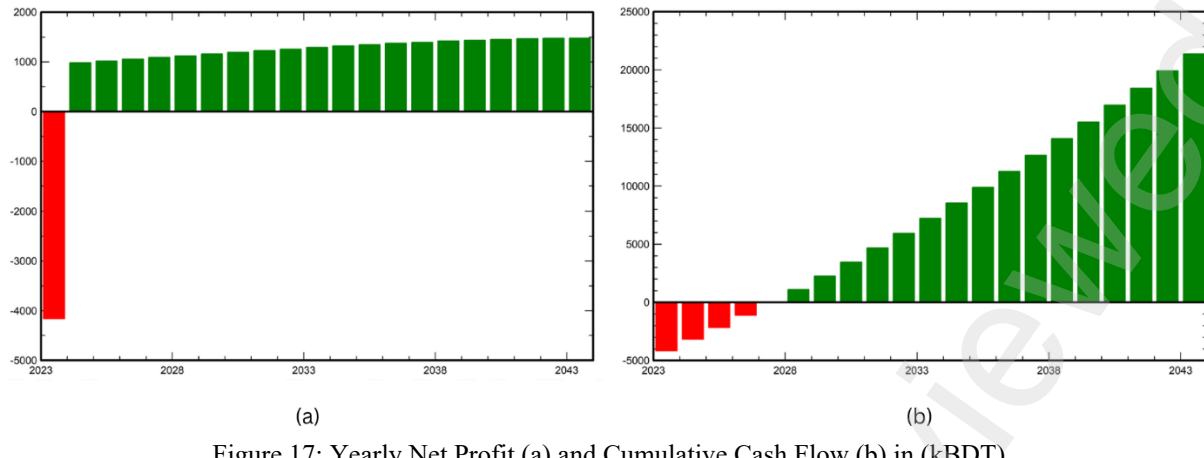


Figure 17: Yearly Net Profit (a) and Cumulative Cash Flow (b) in (kBDT)

Upon completing the simulation, PVsyst generated a summary of the financial parameters, which are detailed in **Table 13**. This summary provides an overview of key financial metrics, offering insights into the project's economic performance and viability.

Table 13: Investment Evaluation using PVsyst

Payback Period	4.1 years
LCOE (BDT/kWh)	11.96
Net Present Value (NPV)	9,010,081 (BDT)
Internal Rate of Return (IRR)	31.43%
Return on Investment (ROI)	216.60%
Paid Dividends	579,627 (BDT)

Formula:

1. $Total Yearly Cost = Operating Cost + Loan Annuities \Rightarrow [Eq 15]$
2. $Production of energy per year, E = A_{module} \times R(\lambda) \times Eff_p \times PR \times 365 \times N_{module} \quad [Eq 16]$
3. $Total specific produce energy, SPE = \frac{E}{TSC} \Rightarrow [Eq 17]$
4. $The Performance Ratio, PR = \frac{E}{E_{collector}} \Rightarrow [Eq 18]$
5. $Payback period, PB = \frac{C_i + C_0}{S_{annual}} \Rightarrow [Eq 19]$

$$a. \quad S_{annual} = \int_{t=0}^{T_{project}} E(t) \times Tariff_{consumption}(t) dt \Rightarrow [Eq 20]$$

Where: $C_0 = Annual Operating Cost$

$$6. \quad Levelized cost of energy, LCOE = \frac{Cost over lifetime}{Total Production over Lifetime} = \frac{\int_{t=0}^{T_{project}} c(t) dt}{\int_{t=0}^{T_{project}} E(t) dt} \Rightarrow [Eq 21]$$

$$7. \quad Net Present Value, NPV = \sum_{t=l}^N \frac{CF_t}{(1 + IRR)^t} - C_i \Rightarrow [Eq 22]$$

Where:

$N = Total number of periods$

$C_i = Initial investment cost (cash outflow at time 0)$

$CF_t = Cash inflow during period t$

$$8. \quad Return on Investment, ROI (\%) = \frac{NPV \times 100\%}{C_i} \Rightarrow [Eq 23]$$

To evaluate the reliability of the simulated data from PVsyst, we will calculate key performance indicators such as performance rating, payback period, LCOE, NPV, and ROI using **Equations 15 to 23**. If the values are mostly below 10%, we can confidently rely on the data provided by PVsyst [42], [43]. As shown in **Table 14**, the error percentage for all the financial parameters are under 10%, suggesting PVsyst data for Swarna Dweep are highly reliable to use as real data [44].

Table 14: Investment Evaluation using Formulas

Parameter	Formula calc.	PVsyst calc.	Unit	Errors %	Remarks on Formulation
E	86,793	92,443	kWh/year	6.11%	Low due to Losses, Resembles PVsyst Results
SPE (System cap. = 60 kW)	1,446.55	1,520	kWh/year	4.83%	Low due to Several Factors
PR ($E_{coll} = 111363 \text{ kWh}$)	77.94	78	%	0.08%	Similar to PVsyst Result
<i>Payback Period</i> ($C_i = 4270375 \text{ BDT}$) ($C_o = 795783.28 \text{ BDT/year}$) ($t = 20 \text{ years}$)	4.9	4.1	Year	18.64%	Various factors were included to lower the consumer cost in PVsyst
S_{annual} (Tariff cons = 12 BDT/kWh)	1,041,516	1,109,316	BDT	6.11%	Similar to PVsyst Result
$LCOE$ ($C_t = 20,186,055 \text{ BDT}$) ($E_t = 1,735,860 \text{ kWh}$)	11.63	11.97	BDT/kWh	2.85%	Similar to PVsyst Result
ROI	204.5	216.6	%	5.59%	Low due to many Financial Factors included in PVsyst
NPV ($IRR = 9\%$)	8,732,347	9,010,081	BDT	3.08%	Similar to PVsyst Result

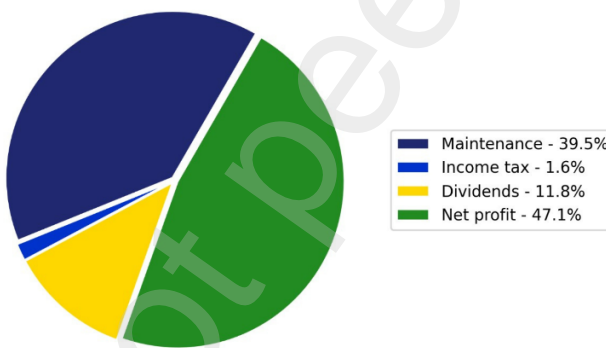


Figure 18: Revenue Distribution Over the Project Lifetime

The pie chart above in **Figure 18** depicts the distribution of a school's net profit across various categories. A significant portion, 39.5%, is allocated to maintenance, highlighting the importance of maintenance and operational efficiency. Dividends account for 11.8% of profits, reflecting the company's commitment to rewarding shareholders. Income taxes cost a modest 1.6%, with the remaining 47.1% retained as net profit. This visual representation provides a clear and concise overview of the institution's financial allocations, making it easy to understand and compare different spending areas.

8. SIA, EIA and Limitations

8.1 Social Impact

The design and implementation of a grid-connected Solar Photovoltaic Power Plant for a school in Swarna Dweep closely align with several Sustainable Development Goals (SDGs), particularly SDG 4 (Quality Education), SDG 7 (Affordable and Clean Energy), SDG 12 (Responsible Consumption and Production), and SDG 13 (Climate Action). This project addresses immediate energy needs while fostering long-term social and economic well-being within the community. By promoting sustainable practices and inclusive growth, the initiative catalyzes broader

sustainable development in Swarna Dweep. The project benefits include improved educational facilities, economic growth, environmental sustainability, health and well-being, and energy independence.

8.2 Environmental Impact

The Environmental Impact Assessment (EIA) of the Solar Photovoltaic Power Plant project in Swarna Dweep highlights critical environmental considerations, including land use and habitat disruption, water resource management, waste management, noise pollution, and community engagement. The regional and global impacts of the project include air quality, water quality, climate change, biodiversity, ecosystem services and energy security. The project is aligned with SDG 13 (Climate Action) and enhances regional energy security by contributing to global climate change mitigation and greenhouse gas emission reduction. Its environmental benefits are significant, establishing a model for sustainable development that can be replicated in remote areas. The project makes a significant contribution to global climate change mitigation by reducing greenhouse gas emissions. The system produces 92.4 MWh annually, with a 0.4% degradation per year. Using the International Energy Agency (IEA) grid emission factor of 584 g CO₂/kWh, the project offsets 961.48 tons of CO₂ over its lifetime—equivalent to 48.074 tons of CO₂ annually which is highlighted in **Figure 19**.

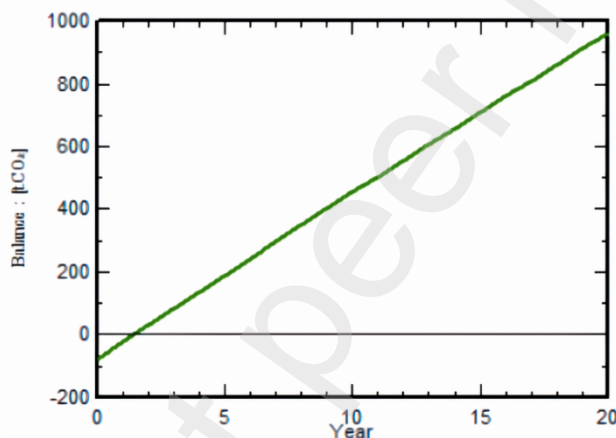


Figure 19: CO₂ Emissions

Table 15 highlights the CO₂ emissions saved by the solar system compared to emissions from different types of power plants, emphasizing its role in reducing greenhouse gas emissions.

Table 15: Annual CO₂ Emissions Savings Compared to Different Fuel Sources

Fuel Source	CO ₂ Emissions (kg CO ₂ /kWh)	Emission Savings (tons)	Ref.
Coal (BIT)	0.9397	86.87	[45]
Natural Gas (CCPP)	0.57	52.7	[46]
Oil Power Plants (CCPP)	0.79	73.03	[46]

Note: Total electricity gen is considered 92,443 kWh/year for CO₂ emissions

This substantial reduction in emissions highlights the critical role renewable energy plays in combating climate change and reducing the global carbon footprint. It contributes directly to international efforts to limit global warming, conforming to IEC 63372.

Table 16: Comparison Between Current Research and Proposed Study

References Vs. Proposed study	Simulation Software	Energy Production	Payback Period (Years)	Panel Rated Power	Performance Ratio, PR (%)	3D modeling and Shadow Analysis
[47]	PVsyst	347 MWh/year	-	250 Wp	75	No
[48]	PVsyst	33.62 MWh/year	-	250 Wp	79.5	Yes
[49]	HOMER Pro	258.75 kWh/year	16.86	330 Wp	-	No
[50]	SketchUp, PVsyst	21,510.186 MWh/year	4.5	500 Wp	84.2	Yes
Proposed study	GSA, PVGIS, PVsyst, SketchUp, AutoCAD	92,443 kWh/year	4.1	620 Wp <i>(BSTI Approved)</i>	78	Yes

A comparison between the existing system and the proposed system, as shown in **Table 16**, reveals several key differences. The proposed system demonstrates greater adaptability and efficiency, addressing critical aspects such as simulation software, energy production, panel selection, 3D design, performance ratio, payback period, and shadow analysis. Unlike the existing study, which often overlooks important factors like performance ratio, payback period, and shadow losses, the proposed system incorporates these elements. By utilizing advanced Mono PERC panels and conducting a comprehensive analysis, the proposed design ensures a more thorough and optimized approach.

8.3 Limitations

The widespread adoption of solar power is hampered by several challenges. Technical limitations include low efficiency and dependence on weather conditions. Infrastructure and land use constraints pose significant barriers, as suitable land is often scarce and solar installations can disrupt ecosystems. High capital costs, equipment shortages, and a lack of skilled labor contribute to financial challenges. The intermittent nature of solar power requires advanced energy storage solutions, which are currently limited and expensive. Finally, regulatory and policy barriers, especially in underserved communities, further hinder the growth of the solar industry. Addressing these challenges is critical for the successful deployment of solar power on a large scale.

9. Conclusion

This assessment presents the design and analysis of a 60 kW grid-connected solar photovoltaic power plant for a school in Swarna Dweep, Bangladesh. The system addresses the critical energy challenges in remote areas by using sustainable solar energy solutions to ensure reliable electricity. The project demonstrated the potential to generate approximately 93,443 kWh annually, with a performance ratio of 0.78, to meet the energy needs of the school while contributing to environmental conservation through significant CO₂ emission reduction. The financial analysis confirmed the viability of the project with a payback period of 4.1 years and an IRR of 31.43%, demonstrating its economic feasibility. The social and environmental benefits emphasize the potential of the project to catalyze socio-economic development consistent with the Sustainable Development Goals. Overall, the project serves as a replicable model for similar educational institutions in remote areas.

10. Future research

Future efforts should focus on integrating real-time monitoring systems and predictive maintenance using advanced data analytics to enhance system efficiency and reliability. Incorporating hybrid energy systems such as wind or biomass can further diversify and stabilize energy supply. In addition, expanding community engagement programs to include training in system operation and maintenance will empower local stakeholders. Detailed environmental impact assessments, combined with improved weather forecasting, can optimize system designs for different climate conditions. Finally, policy advocacy and exploring financial risk mitigation strategies can strengthen the framework for renewable energy adoption in similar projects in Bangladesh and beyond.

CRediT authorship contribution statement

Ayman Khan: Writing – original draft, Methodology, Software, Formal analysis, Data curation, Validation, Conceptualization. **Abdullah Al Masud:** Writing – review & editing, Software, Drawing, Visualization, Conceptualization. **Tarek Ahmed:** Writing – original draft, Methodology, Data curation, Conceptualization. **Nabil Mohammad Chowdhury:** Supervision, Formal analysis, Resources, Project administration, Funding acquisition.

Declaration of competing interest

The authors declare that they have no known competing financial interests or personal relationships that could have appeared to influence the work reported in this paper.

Data availability

Data will be made available on request.

Acknowledgment

This research was not funded by any grant.

Supplementary materials

Supplementary material associated with this article can be found, in the online version, at doi:10.1016/j.nexus.2024.100286.

References

- [1] “Renewable energy: Prospects and trends in Bangladesh,” *Renewable and Sustainable Energy Reviews*, vol. 70, pp. 44–49, Apr. 2017.
- [2] “Fossil fuel sustainability index: An application of resource management,” *Energy Policy*, vol. 35, no. 5, pp. 2969–2977, May 2007.
- [3] A. Shahsavari and M. Akbari, “Potential of solar energy in developing countries for reducing energy-related emissions,” *Renew. Sustain. Energy Rev.*, vol. 90, pp. 275–291, Jul. 2018. [Online]. Available: <https://doi.org/10.52132/Ajrsp.e.2023.52.3>
- [4] “A comprehensive review of automatic cleaning systems of solar panels,” *Sustainable Energy Technologies and Assessments*, vol. 47, p. 101518, Oct. 2021.
- [5] N. M. Kumar, M. S. P. Subathra, and J. E. Moses, “On-grid solar photovoltaic system: Components, design considerations, and case study,” in *2018 4th International Conference on Electrical Energy Systems (ICEES)*, IEEE, Feb. 2018. doi: 10.1109/icees.2018.8442403.
- [6] “Factors responsible for solar PV adoption at household level: A case of Lahore, Pakistan,” *Renewable and Sustainable Energy Reviews*, vol. 78, pp. 754–763, Oct. 2017.
- [7] M. A. Rahman, M. Islam, and M. T. Islam, “Design of a 40 MW Grid-Connected Solar Photovoltaic Power Plant for a School in Patenga,” Apr. 2024, doi: 10.21203/rs.3.rs-4301542/v1.
- [8] “Assessment of solar energy technologies in Africa-opportunities and challenges in meeting the 2030 agenda and sustainable development goals,” *Energy Policy*, vol. 137, p. 111180, Feb. 2020.
- [9] “The dynamics of solar PV costs and prices as a challenge for technology forecasting,” *Renewable and Sustainable Energy Reviews*, vol. 26, pp. 96–107, Oct. 2013.
- [10] S. S. Sadrul Huda, “Increasing green footprints: Indications of transformations in the socio-economic spaces of Bangladesh,” *Engineering Reports*, vol. 6, no. 1, p. e12775, Jan. 2024.
- [11] M. K. Amin, K. M. Anik Rahaman, and M. Nujhat, “Assessment of erosion-accretion patterns, land dynamics, and climate change impacts on the islands of the south-central coastal zone of Bangladesh using remote sensing techniques,” *Marine Geodesy*, Nov. 2024, doi: 10.1080/01490419.2024.2388321.
- [12] M. Sengupta, A. Habte, S. Wilbert, C. Gueymard, and J. Remund, “Best Practices Handbook for

- the Collection and Use of Solar Resource Data for Solar Energy Applications: Third Edition," National Renewable Energy Lab. (NREL), Golden, CO (United States), NREL/TP-5D00-77635, Apr. 2021. doi: 10.2172/1778700.
- [13] S. Shirzad, A. M. Fazli, W. Zgham, and S. A. Z. Fatemi., "Design and development of grid-connected solar PV power plant using PVsyst," *Academic Journal of Research and Scientific Publishing*, vol. 5, no. 52, pp. 67–86, Aug. 2023.
- [14] J. Assadeg, K. Sopian, and A. Fudholi, "Performance of grid-connected solar photovoltaic power plants in the Middle East and North Africa," *Int. J. Electr. Comput. Eng. (IJECE)*, vol. 9, no. 5, p. 3375, Oct. 2019.
- [15] G. R. Krishna, B. Krishna Nallamothu, R. Janga, and S. R. Pendem, "Design of 400KWP grid connected solar PV system for bapatla engineering college," in *2023 Second IEEE International Conference on Measurement, Instrumentation, Control and Automation (ICMICA)*, IEEE, May 2024, pp. 1–6.
- [16] A. Trivaldo, F. Husin, and R. Gianto, "Planning study of on-grid based solar power plant at senior high school of Negeri 1 meliau," *Journal of Electrical Engineering, Energy, and Information Technology (J3EIT)*, vol. 12, no. 1, p. 279, Apr. 2024.
- [17] "Design, simulation and economic evaluation of 90 kW grid connected Photovoltaic system," *Energy Reports*, vol. 6, pp. 1778–1787, Nov. 2020.
- [18] A. N. Akpolat, E. Dursun, A. E. Kuzucuoğlu, Y. Yang, F. Blaabjerg, and A. F. Baba, "Performance analysis of a grid-connected rooftop solar photovoltaic system," *Electronics (Basel)*, vol. 8, no. 8, p. 905, Aug. 2019.
- [19] I. Gharibshahian, S. Sharbati, and A. Orouji, "The design and evaluation of a 100 kW grid connected solar photovoltaic power plant in Semnan city," *Journal of Solar Energy Research*, vol. 2, no. 4, pp. 287–293, Oct. 2017.
- [20] B. P. Mohanty and M. Srivalli, "Optimization and design of grid connected rooftop solar power plant under various operating conditions," in *2020 International Conference on Computational Intelligence for Smart Power System and Sustainable Energy (CISPSSE)*, IEEE, Jul. 2020. doi: 10.1109/cispsse49931.2020.9212254.
- [21] N. Aoun, "Energy and exergy analysis of a 20-MW grid-connected PV plant operating under harsh climatic conditions," *Clean Energy*, vol. 8, no. 1, pp. 281–296, Feb. 2024.
- [22] I. Raxmatov, K. Samiyev, and M. Mirzayev, "Analysis of the efficiency of 300 kw grid-connected solar photovoltaic systems at Bukhara state university," *BIO Web of Conferences*, vol. 84, p. 05020, 2024.
- [23] Abdullah, M. Putri, and J. Iriani, "Analysis of the effect of tilt position and surface temperature levels of solar panels in optimizing solar panel performance," *Int J Res Rev*, vol. 10, no. 12, pp. 372–380, Dec. 2023.
- [24] H. Ahn, "A framework for developing data-driven correction factors for solar PV systems," *Energy (Oxf.)*, vol. 290, no. 130096, p. 130096, Mar. 2024.
- [25] A. Kowsar, S. C. Debnath, N. Haque, M. S. Islam, and F. Alam, "Design of a 100 MW solar power plant on wetland in Bangladesh," in *3RD INTERNATIONAL CONFERENCE ON ENERGY AND POWER, ICEP2021*, AIP Publishing, 2022. doi: 10.1063/5.0114976.
- [26] A. J. Kil and T. C. J. van der Weiden, "Performance of modular grid connected PV systems with undersized inverters in Portugal and the Netherlands," in *Proceedings of 1994 IEEE 1st World Conference on Photovoltaic Energy Conversion - WCPEC (A Joint Conference of PVSC, PVSEC and PSEC)*, IEEE, 2002. doi: 10.1109/wcpec.1994.520136.
- [27] F. Blaabjerg and E. Koutroulis, "Methods for the optimal design of grid-connected PV inverters," *International Journal of Renewable Energy Research*, vol. 1, no. 2, pp. 54–64, 2011.
- [28] Y.-M. Saint-Drenan and T. Barbier, "Data-analysis and modelling of the effect of inter-row shading on the power production of photovoltaic plants," *Sol. Energy*, vol. 184, pp. 127–147, May 2019.
- [29] C. Barreiro, P. M. Jansson, A. Thompson, and J. L. Schmalzel, "PV by-pass diode performance in landscape and portrait modalities," in *2011 37th IEEE Photovoltaic Specialists Conference*, IEEE, Jun. 2011. doi: 10.1109/pvsc.2011.6186599.
- [30] A. Khelifa and M. Bounib, "Intelligent method optimization for improve heat transfer in solar hybrid collector." Accessed: Dec. 04, 2024. [Online]. Available:

<https://doi.org/10.1109/ICRSEtoSET56772.2023.10525485>

- [31] F. C. Krebs, H. Spanggard, T. Kjær, M. Biancardo, and J. Alstrup, "Large area plastic solar cell modules," *Mater. Sci. Eng. B Solid State Mater. Adv. Technol.*, vol. 138, no. 2, pp. 106–111, Mar. 2007.
- [32] V. L. Mishra, Y. K. Chauhan, and K. S. Verma, "A comprehensive investigation of a solar array with wire length under partial shading conditions," *Energy Sources Recovery Util. Environ. Eff.*, vol. 45, no. 4, pp. 10217–10241, Oct. 2023.
- [33] P. Paul Gyang, Department of Electrical & Electronics Engineering, University of Lagos, Nigeria, F. E. Alfred-Abam, and F. P. Olubodun, "Analysis of an actively energized 11/0.415 kV distribution transformer using power quality and energy analyzer," *Int. J. Eng. Manuf.*, vol. 13, no. 3, pp. 1–9, Jun. 2023.
- [34] H. Liu, Z. Zhang, J. Zhang, X. Huang, Z. Wang, and L. Zhao, "Study on winding looseness of power transformer based on vibration," *IOP Conf. Ser. Mater. Sci. Eng.*, vol. 486, no. 1, p. 012032, Jun. 2019.
- [35] C. M. Coman, A. Florescu, and C. D. Oancea, "Improving the efficiency and sustainability of power systems using distributed power factor correction methods," *Sustainability*, vol. 12, no. 8, p. 3134, Apr. 2020.
- [36] W. H. Preece, "I. On the heating effects of electric currents. No. II," *Proc. R. Soc. Lond.*, vol. 43, no. 258–265, pp. 280–295, Dec. 1888.
- [37] W. H. Preece, "IV. On the heating effects of electric currents. No. III," *Proc. R. Soc. Lond.*, vol. 44, no. 266–272, pp. 109–111, Dec. 1888.
- [38] "Voltage Drop Calculations," Mar. 21, 2022, Wiley. doi: 10.1002/9783527803422.ch16.
- [39] N. H. Reich, B. Mueller, A. Armbruster, W. G. J. H. M. van Sark, K. Kiefer, and C. Reise, "Performance ratio revisited: is PR > 90% realistic?: Performance ratio revisited: is PR > 90% realistic?," *Prog. Photovolt.*, vol. 20, no. 6, pp. 717–726, Sep. 2012.
- [40] *Journal of energy research and reviews*. Sciencedomain International, 2019. doi: 10.9734/jenrr.
- [41] S. Lindig, D. Moser, A. J. Curran, and R. H. French, "Performance Loss Rates of PV systems of Task 13 database," in *2019 IEEE 46th Photovoltaic Specialists Conference (PVSC)*, IEEE, Jun. 2019. doi: 10.1109/pvsc40753.2019.8980638.
- [42] M. Nazififard, H. Hashemi-Dezaki, and K. Nazififard, "Comparing actual measurement and PvSyst simulation results for energy generation of microgrid-connected PV systems," in *2023 13th Smart Grid Conference (SGC)*, IEEE, Dec. 2023, pp. 1–6.
- [43] T. Betti, I. Bevanda, I. Marasović, and I. Zulim, "A new approach to comparing photovoltaic simulation software," *Energy Sources Recovery Util. Environ. Eff.*, vol. 45, no. 2, pp. 6290–6304, Jun. 2023.
- [44] Z. C. Viana, J. dos Santos Costa, J. V. Silva, and R. Martins Fernandes, "Accuracy analysis of pvsyst software for estimating the generation of a photovoltaic system at the polo de inovação Campos dos goytacazes," in *2020 IEEE PES Transmission & Distribution Conference and Exhibition - Latin America (T&D LA)*, IEEE, Sep. 2020. doi: 10.1109/tvla47668.2020.9326203.
- [45] H. Cai, M. Wang, A. Elgowainy, and J. Han, "Updated greenhouse gas and criteria air pollutant emission factors and their probability distribution functions for electricity generating units," Office of Scientific and Technical Information (OSTI), Jul. 2012. doi: 10.2172/1045758.
- [46] M. Hauck, Z. J. N. Steinmann, A. M. Schipper, F. Gorrisen, A. Venkatesh, and M. A. J. Huijbregts, "Estimating the greenhouse gas balance of individual gas-fired and oil-fired electricity plants on a global scale: Greenhouse gas balance of individual power plants," *J. Ind. Ecol.*, vol. 21, no. 1, pp. 127–135, Feb. 2017.
- [47] O. A. Ahmed, W. H. Habeeb, D. Y. Mahmood, K. A. Jalal, and H. K. Sayed, "Design and performance analysis of 250 kW grid-connected photovoltaic system in Iraqi environment using PvSyst software," *Indones. J. Electr. Eng. Inform. (IJEI)*, vol. 7, no. 3, Aug. 2019, doi: 10.52549/ijeei.v7i3.978.
- [48] A. Chauhan, M. Sharma, and S. Baghel, "Designing and performance analysis of 15KWP grid connection photovoltaic system using pvsyst software," in *2020 Second International Conference on Inventive Research in Computing Applications (ICIRCA)*, IEEE, Jul. 2020. doi: 10.1109/icirca48905.2020.9183386.
- [49] D. M. Mahmud, S. M. M. Ahmed, S. Hasan, and M. Zeyad, "Grid-connected microgrid: design

- and feasibility analysis for a local community in Bangladesh," *Clean Energy*, vol. 6, no. 3, pp. 447–459, Jun. 2022.
- [50] M. H. Nabil *et al.*, "Techno-economic analysis of commercial-scale 15 MW on-grid ground solar PV systems in Bakalia: A feasibility study proposed for BPDB," *Energy Nexus*, vol. 14, no. 100286, p. 100286, Jul. 2024.

Biographies

Ayman Khan is completing his Bachelor's degree in Mechanical Engineering at Ahsanullah University of Science and Technology. His academic and research interests include renewable energy systems, automation, computational mechanics, and material behavior. With a strong passion for design and development, he has contributed significantly to research, including a study on an RFID module enhanced with a thermophile sensor for door mechanisms, which was recognized as a proceeding at an IEOM Society conference and awarded 1st runner-up in project competition. He has authored a book chapter on waste-derived molecular imprinting carbonaceous nanomaterials, under review for publication by Wiley, and is working on another chapter focusing on biopolymer-based hydrogel with electrostatic reinforcement for bone regeneration, to be published by Elsevier. Orcid ID: <https://orcid.org/0009-0002-0184-7265>

Abdullah Al Masud is completing his undergraduate studies at Ahsanullah University of Science and Technology (AUST), Dhaka, pursuing a Bachelor of Science in Mechanical Engineering (ME) through the Department of Mechanical and Production Engineering (MPE), accredited by BAETE. Recently, he completed conference for ICMMPE-2024 at DUET and IEOM-2024 at AIUB as the first author of the papers related to Bagasse Fiber-Reinforced Materials. His academic journey has instilled in him a strong foundation in engineering principles, which he is now actively applying in the field of composite materials. Driven by a passion for integrity, excellence and innovation, Masud aspires to become an eminent mechanical engineer. He is particularly keen to secure a role in the research and development (R&D) sector, where he can utilize his skills and knowledge to advance engineering. Orcid ID: <https://orcid.org/0009-0000-6784-0395>

Tarek Ahmed is completing his Bachelor of Science in Mechanical Engineering at Ahsanullah University of Science and Technology (AUST), Dhaka, Bangladesh. His academic and research interests include renewable energy systems, machine learning, computational mechanics, and material behavior. For his undergraduate thesis, Tarek utilized machine learning techniques to predict wind and solar power generation, addressing critical challenges like energy intermittency, grid stability, and resource optimization, integrating weather and energy data to enhance renewable energy reliability. He worked on optimizing airfoils for horizontal axis wind turbines, focusing on lift, drag, and efficiency improvements at a Reynolds number of 400,000, inspired by the NACA 6412 airfoil. Notably, Tarek's project on IoT-based RFID security systems, which integrates RFID technology with temperature sensors for enhanced security and safety applications, is being published in a conference. His other work includes designing a lead screw for machining applications, incorporating stress and torque analyses to ensure precision and durability. Proficient in tools like SolidWorks, ANSYS, Python, and advanced programming frameworks, Tarek is committed to advancing sustainable energy solutions and innovative engineering designs, aspiring to make significant contributions to both academia and industry. Orcid ID: <https://orcid.org/0009-0008-3904-2781>

Nabil Mohammad Chowdhury is a Lecturer in Mechanical Engineering (ME) program under the Department of Mechanical and Production Engineering at Ahsanullah University of Science and Technology (AUST). He has actively contributed to the field of heat transfer and thermal system optimization through his research on advanced heat sink designs. His recent publication in the renowned journal *Helijon* (Q1, IF: 3.4) focuses on the "Optimization of hydrothermal performance in industrial heat sinks with innovative perforated pin fin designs: A numerical approach." This work presents a cutting-edge numerical analysis that enhances the efficiency of industrial heat sinks. Additionally, Nabil has authored another significant study, published by Elsevier, titled "A novel pin finned structure-embedded microchannel heat sink: CFD-data driven MLP, MLR, and XGBR machine learning models for thermal and fluid flow prediction." This research integrates computational fluid dynamics

(CFD) with advanced machine learning models, providing a comprehensive solution for predicting the thermal and fluid flow performance of microchannel heat sinks.